CRYSTAL GROWTH & DESIGN

pubs.acs.org/crystal

Perspective

Chocolate Tempering: A Perspective

Jarvis A. Stobbs, Saeed M. Ghazani, Mary-Ellen Donnelly, and Alejandro G. Marangoni*

Cite This: *Cryst. Growth Des.* 2025, 25, 2764–2783

Read Online

ACCESS | Metrics & More | Article Recommendations

ABSTRACT: Tempering is a critical step in chocolate production, ensuring desirable properties such as gloss, snap, and bloom resistance. Traditionally, tempering has been understood through the lens of cocoa butter polymorphism, with a predominant focus on achieving Form V crystals, due to their sharp melting profile and associated macroscopic physical properties. However, this Perspective challenges the notion that Form V alone guarantees high-quality, bloom-resistant chocolate. Recent research suggests that polymorphism is only one aspect of chocolate quality. Multiscale structural analyses—including small-angle X-ray scattering (SAXS), ultrasmall-angle X-ray scattering (USAXS), small-angle neutron scattering (SANS), and microcomputed tomography (μCT)—reveal that nanostructural to microstructural properties are key indicators of bloom susceptibility and can vary significantly, despite identical polymorphic phases. This Perspective proposes that tempering should be viewed as a hierarchical crystallization process, where nucleation rate, structural homogeneity, and microstructural organization play critical roles. A broader approach to tempering assessment—integrating microstructural probes alongside traditional solid-state characterization—may provide deeper insights into chocolate's mechanical stability and long-term bloom resistance. As supply chain fluctuations increasingly impact cocoa butter composition, this multiscale perspective could help manufacturers mitigate quality inconsistencies and adapt to cost-driven formulation changes that may otherwise compromise bloom resistance in tempered chocolate.

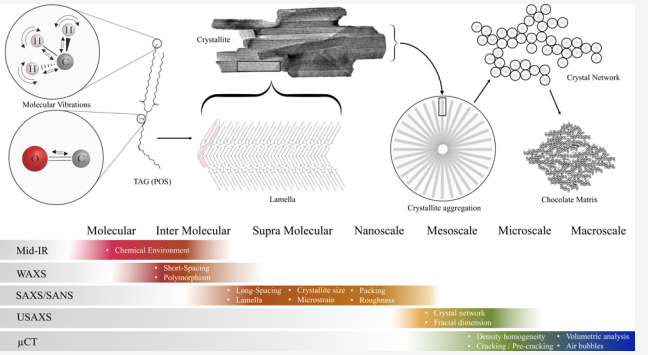

INTRODUCTION: HISTORY OF CHOCOLATE, POLYMORPHISM, TEMPERING, AND ANALYSIS TOOLS

Herein, we present a perspective on the structural complexity of chocolate tempering, emphasizing the role of multiscale crystallization beyond the conventional focus on cocoa butter polymorphism. Despite decades of research and extensive industrial practice, conventional approaches to chocolate tempering—focusing exclusively on achieving Form V polymorphism—have proven insufficient to fully address persistent issues such as fat bloom and microstructural instability. In developing this Perspective, we pay homage to the pioneering work that has laid the foundation for our current understanding of chocolate tempering, acknowledging the collective efforts that have brought us to where we are today.

The evolution of chocolate over the centuries has been truly remarkable. Early preparations in Central America before the 1800s—where Indigenous peoples used whole cacao beans, sugar, and spices to create chocolate drinks—contrast with today's focus on sustainable, ethical sourcing and the production of plant-based, premium, and artisan chocolates. Despite these dramatic changes, the physical and sensory attributes of chocolate have remained closely tied to its key ingredients.

Chocolate primarily consists of four main ingredients: cocoa butter (CB), sugar, cocoa nibs, and lecithin. Among these, CB plays a crucial role in defining the product's physical and sensory attributes—such as its snap, gloss, firmness, and sharp melting behavior—because these properties depend on the intricate crystallization of CB. Cocoa nibs, which comprise approximately 55% CB on a dry basis,[1] serve as the principal source of fat in chocolate formulations. Cocoa butter is a complex molecular mixture of predominantly triacylglycerols (TAGs), including 1,3-dipalmitoyl-2-oleoyl-*sn*-glycerol (POP), 1-palmitoyl-2-oleoyl-*sn*-3-stearoyl-glycerol (POS), and 1,3-distearoyl-2-oleoyl-*sn*-glycerol (SOS), which together account for over 80% of its TAG content.[2,3] The unique characteristics of CB arise mainly from the polymorphism of these TAGs and their interactions with other minor components found in the source CB. Notably, the level of minor components in CB is relatively high compared to other lipids used in food products

Received: February 28, 2025
Revised: April 3, 2025
Accepted: April 3, 2025
Published: April 16, 2025

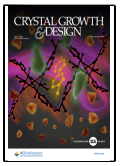

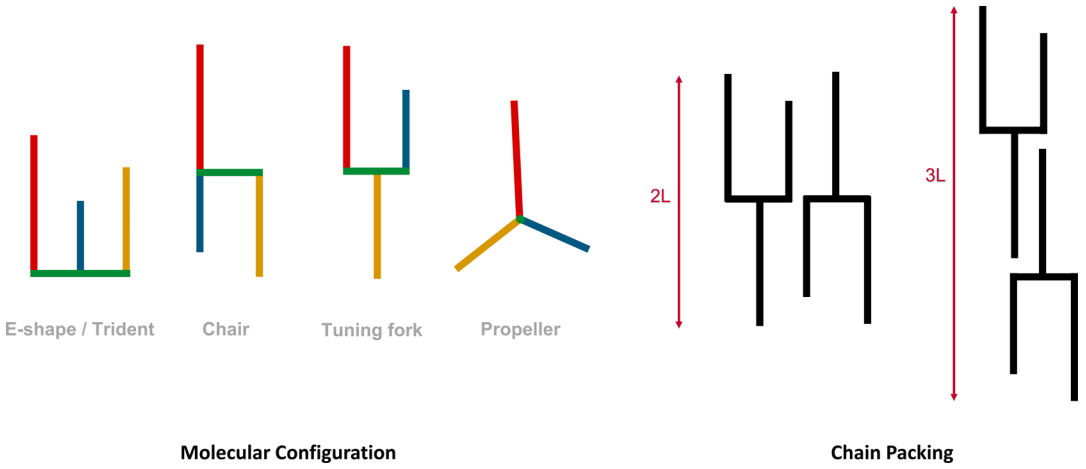

Figure 1. Molecular configuration that can be adopted by triacylglycerols, and their typical stacking configurations, 2L and 3L.

such as vegetable oils, contributing further complexity to its crystallization behavior. These levels can also be affected by postextraction refining processes such as steam-distillation/deodorization or bleaching, which may alter the crystallization behavior by removing or modifying key minor compounds.

In general, polymorphism refers to the ability of a chemical substance to crystallize into multiple distinct crystal structures while retaining the same chemical composition. This phenomenon arises due to variations in crystallization conditions, leading to different molecular arrangements within the crystal lattice. As a result, polymorphs can exhibit unique physical and physicochemical properties, including differences in melting point, solubility, stability, and mechanical strength. Physicochemical properties reflect how molecular arrangement (physical structure) arises from the underlying chemistry and, in turn, influences material characteristics such as texture and melting behavior. These variations are crucial in determining a material's performance across various applications and central in a chocolate confection.

Today, it is known that the polymorphic behavior of CB is governed by the molecular structure of its constituent TAGs, which are influenced by fatty acid chain length, degree of unsaturation, and stereochemistry.[4] However, the nomenclature and consistency in how this is described in the literature can vary. Here, we will summarize the key concepts from molecular structure to the various polymorphisms of CB. First the molecular structure of a given TAG can fall into three general conformations and commonly described as E/trident-shaped, chair-shaped, tuning-fork-shaped, or propeller-shaped (Figure 1). These conformations, in turn, dictate how TAGs pack together and form ordered crystalline structures.

The mixture of TAGs found in CB can crystallize into three of the seven known crystalline families, namely hexagonal, orthorhombic, and triclinic, and are designated as α, β', and β, respectively, each exhibiting distinct molecular order and stability.[5] The α-form represents a loosely packed, unstable phase with rapid crystallization kinetics, while the β'-form exhibit a more ordered arrangement but remain less stable than the β-form, which is the most thermodynamically stable. These transitions follow a monotropic sequence, wherein decreasing Gibbs energy favors the transformation from $\alpha \rightarrow \beta' \rightarrow \beta$.[5]

Each of these crystalline families is further characterized by its lamellar stacking arrangement, which refers to the way TAG molecules are organized in layers. Two primary crystal stacking modes exist for TAGs in CB: bilayer (2L) and trilayer (3L) packing[6] (Figure 1). This supramolecular arrangement is not usually associated with polymorphism, per se. Polymorphism refers to the packing of the carbon atoms in the long hydrocarbon-like chains in TAGs, while this stacking arrangement of whole TAG molecules has been referred to as "polytypism".[7] The origin of this nomenclature is rather historical, mirroring development in powder XRD. In reality, each of the polymorphs in cocoa butter represents a unique crystal form of specific symmetry. This concept, however, has not evolved sufficiently yet, and we are left with the old scheme of naming polymorphs referring to a "subcell" within the unit cell and a stacking arrangement related to the dimension of the long axis of the TAG unit cell. In our view, once Rietveld refinement improves and actual solid data on TAG crystals starts being available in the literature, a rethinking of the classification of TAG crystal forms needs to take place. Until then, we are left with α, β', β, and 2L and 3L.

In general, for TAGs, 2L packing refers to a bilayer structure in which the acyl chains of the TAG molecules are arranged in a near-parallel fashion with chains repeating every two molecules. This packing mode is typically associated with a "homogeneous" configuration, such as SSS (saturated fatty acids at all three stereospecific positions [*sn*]) TAGs, where the chains' regularity permits efficient packing into a 2-layer bilayer. On the other hand, 3L packing involves a staggered arrangement of acyl chains in which each chain repeats every three molecules, and is typically associated with the formation of a triclinic unit cell structure in model TAG systems. This packing arrangement is characteristic of the β polymorphs, which represent the most thermodynamically stable forms of SUS-type (saturated fatty acids at *sn*-1 and *sn*-3 and unsaturated at *sn*-2) TAGs. In the context of CB, POP, POS, and SOS have the SUS configuration and this asymmetry in SUS TAGs results in the disruption of the bilayer structure and requires the system to adopt a more-stable 3L arrangement to accommodate the altered molecular geometry.

Given this framework, it is generally agreed that CB can be divided into six polymorphic types, designated I–VI. Namely, Form I is referred to as the sub-α, Form II as the α, Form III as the β_2', Form IV as the β_1', Form V as the β_2, and Form VI as the β_1. These types correspond to varying degrees of stability, melting points, and textural properties. Forms I and II are generally regarded as unstable, readily transforming into higher

https://doi.org/10.1021/acs.cgd.5c00269
Cryst. Growth Des. 2025, 25, 2764−2783

Table 1. Cocoa Butter Polymorphs, Forms, Crystal Family, Lamella Stacking, and Melting Ranges[a]

polymorph	form	crystal family	symbol	lateral packing	melting temperature (°C)
sub-α	I	hexagonal	H	2L	13.0−18.0
α	II	hexagonal	H	2L	17.1−24.0
β_2'	III	orthorhombic perpendicular	O⊥	2L	22.4−28.0
β_1'	IV	orthorhombic perpendicular	O⊥	2L	21.0−33.0
β_2	V	triclinic	T//	3L	30.0−34.5
β_1	VI	triclinic	T//	3L	33.5−38.5

[a]Data taken from refs 3 and 9.

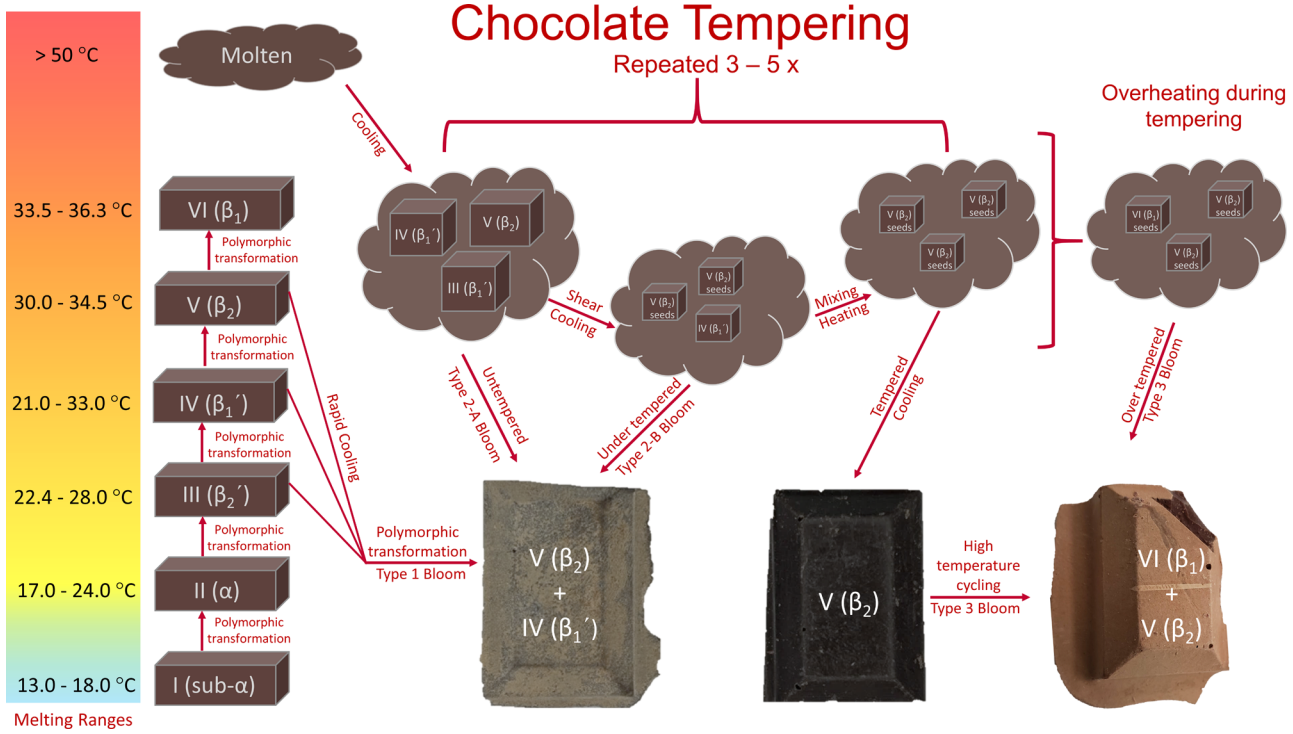

Figure 2. Chocolate tempering schematic. Rapid cooling leads to the formation of unstable polymorphs that undergo rapid polymorphic transitions, leading to Type 1 bloom. Untempered and under-tempered chocolate result in Type 2-A and Type 2-B bloom, respectively. Overtempered chocolate, created due to improper storage and exposure to temperature cycles of high temperature, produces Type 3 bloom and typically occurs over extended periods of time.

forms under typical processing or storage conditions. Forms III, IV, and V are considered metastable—they are kinetically stable enough to persist for extended periods but are not the thermodynamic minimum and will gradually transform into more stable forms if conditions allow. Form VI is the only thermodynamically stable polymorph, possessing the lowest Gibbs energy, although it is typically undesirable in chocolate due to its association with fat bloom and brittle texture. Form V (β_2) is particularly noteworthy for chocolate production. This polymorph exhibits a well-ordered 3L-triclinic structure with an optimal melting behavior near body temperature (~30.0−34.5 °C), which contributes to chocolate's characteristic snap, smooth texture, and resistance to fat bloom. Literature often uses inconsistent or mixed nomenclature in the identification of CB structures. Table 1 lists these various nomenclatures for the polymorphic forms of CB TAGs, along with their associated melting points, crystal families, and lamellar packing. The α-form, typically identified as 2L, has been reported to occasionally adopt a 3L structure in dairy-free milk chocolates, although this is not commonly observed or reported.[8] It should be noted that the melting temperatures are highly dependent on the specific composition of TAGs within the CB. Variations in the relative proportions of TAGs—specifically POP, POS, SOS, and a multitude of minor components—lead to significant differences in melting ranges. The ranges of various polymorphic forms tend to overlap, necessitating source-specific characterization.

The phenomenon of polymorphism in CB has been a subject of rigorous study and, at times, controversy. Early work identified the multiple melting points and the number of polymorphs present in CB. Loskit first reported three polymorphs in 1928; later, in 1951, Vaeck identified four distinct forms; in 1964, Duck provided evidence for five polymorphic forms; and Wille and Lutton expanded the classification to six polymorphic forms in 1966.[10−12] There is strong debate and conflicting research on if there are truly 6 forms or whether some classifications of the different polymorphisms are mixtures and referred to as pseudoforms. Regardless, it was therefore determined decades ago that among different polymorphs, only Form V is desirable for chocolate. To obtain this polymorphic form, the tempering process, the most critical step in chocolate manufacturing, is designed to crystallize CB into Form V with the appropriate number, shape, and size of crystals.[13]

https://doi.org/10.1021/acs.cgd.5c00269
Cryst. Growth Des. 2025, 25, 2764−2783

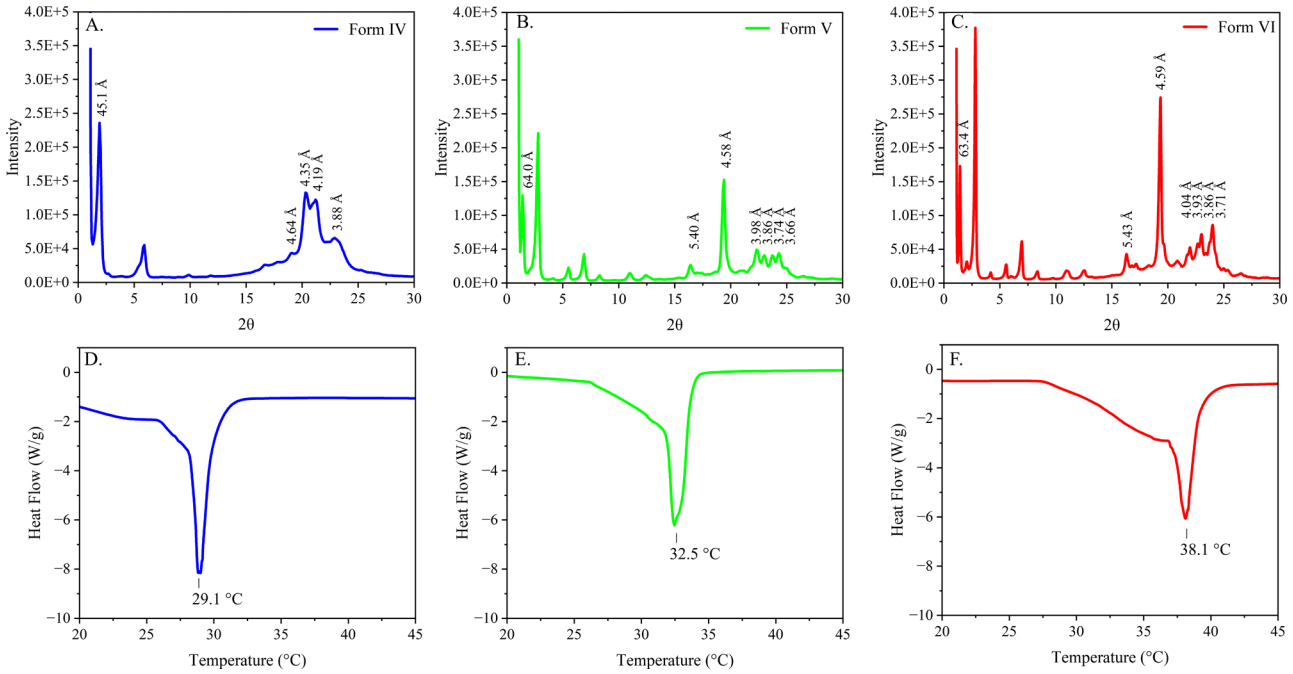

Figure 3. Representative (A−C) wide-angle X-ray scattering patterns and (D−F) differential scanning calorimetry curves of Forms IV, V, and VI polymorphs in cocoa butter.

Tempering is a controlled process of heating and cooling chocolate to achieve a stable crystalline structure in CB, which is essential for producing chocolate with a smooth texture, glossy appearance, and desirable snap. Although the term "tempering" is also used in metallurgy, where it refers to heat treatment used to alter hardness or ductility, chocolate tempering is fundamentally different. In this context, tempering refers specifically to the manipulation of cocoa butter polymorphism to ensure the formation of the desirable Form V (β_2) polymorph, which is associated with optimal physical and sensory properties.

First, the chocolate is melted to fully dissolve all fat crystals. The exact temperature varies depending on the type of chocolate—dark, milk, or white. Using dark chocolate as an example, it is heated past 50 °C, often to 60 °C, until fully melted. Precrystallization is then initiated by cooling under controlled stirring (shear), which plays a critical role in promoting uniform crystallization and facilitating the formation of seed crystals. In dark chocolate, this cooling step typically occurs around 27−29 °C. Shear also helps to distribute the newly formed crystals, which will be a mixture of primarily Form IV and V. Next, the chocolate is gently reheated to just below the melting point of Form V crystals, around 31−32 °C, to remove any remaining unstable forms primarily Form IV without dissolving/melting the desired form V crystals. The chocolate is again allowed to cool and the Form V crystals act as nucleation points for further Form V crystallization. Sometimes, tempered chocolate that already contains Form V crystals can be added to the melted chocolate. This technique, known as seeding, accelerates the formation of the desired crystalline structure, improves consistency in the final product, and may reduce the number of tempering cycles needed. This reheating and cooling cycle is often repeated 3−5 times to ensure a well-tempered chocolate with uniform crystal distribution and content of about 2 − 5% Form V crystals and a schematic can be seen in Figure 2. The tempering temperatures and times depend on the origin and chemical composition of CB, making this process uniquely different, depending on where CB is sourced.[14] Therefore, bloom may occur under the same processing conditions when different CB sources are used.[14]

Previous studies have shown that improper tempering can lead to bloom development in chocolate, a physical phenomenon caused by the polymorphic transition of CB crystals. The underlying causes of bloom development in chocolate are numerous, and so far, not completely elucidated. In 1956, Becker suggested that bloom development during chocolate storage is due to the phase separation of low-melting TAGs 1-palmitoyl-2,3-dioleyl-*sn*-glycerol (POO) and 1-stearoyl-2,3-dioleyl-*sn*-glycerol (SOO) from high-melting TAGs (POP, POS, and SOS) within the crystalline structure of CB.[15] Five years later, Kleinert rejected this hypothesis, indicating that fast-cooling chocolate leads to the formation of metastable crystal forms in chocolate leading to bloom development.[16] In 1966, Wille and Lutton first proposed the recrystallization of CB crystals from a less-stable form to a more-stable polymorph leading to the formation of whitish haze on chocolate.[10] Later, in 1988, Schlichter-Aronhime and Garti argued that in CB, Form IV is a purified variant of Form V—not a polymorphic form—and that this purified form is responsible for blooming.[17]

In 2012, Kinta and Hatta[18] published the combined work and classified 4 distinct forms of bloom in chocolate, namely Type 1, Type 2-A, Type 2-B, and Type 3. In Type 1 bloom, 2001 Sato and Koyano[19] have shown that fat separation occurs concurrently with the polymorphic transition of CB, involving shifts from unstable crystals to Form V and further from Form V to Form VI. Importantly, the occurrence of fat separation is not restricted to any single transition. In 1998 Bricknell and Hartel[20] documented cases where the transition from Form V to VI did not result in bloom. These observations indicate that

https://doi.org/10.1021/acs.cgd.5c00269
Cryst. Growth Des. 2025, 25, 2764−2783

bloom Type 1 in tempered chocolate may emerge from several transitions including III → IV, IV → V, or V → VI.

Type 2-A bloom develops when chocolate solidifies without the presence of Form V crystals. In such cases, spherical dark brown parts are observed in the chocolate and have been identified as Form V.[21] This type, predominantly found in untempered chocolate, involves transitions mainly from Forms III and IV to V, where the absence of seed crystals leads to uneven fat distribution. Type 2-B bloom similarly occurs when Form V crystals are present but are insufficient quantity for complete tempering and form in under tempered chocolate. Although the details are less explicitly outlined, available evidence suggests that this bloom type is primarily associated with Form IV to V transitions.[22]

Type 3 bloom, however, can occur in two ways. Initially, when CB crystals are heated just below their melting point, partial melting induces a gradual, oil-mediated transformation from Form V to Form VI.[19] Therefore, during the tempering process, high or excessive temperature cycling—or improper storage with such exposure—can lead to repetitive partial melting and recrystallization, promoting the formation of Form VI crystal and/or the separation for high melting point TAGs and polymorphs (Forms V and VI). Thus, Type 3 bloom is mainly associated with Form VI, though it can also involve Form V. Overall, these findings demonstrate that chocolate bloom is not solely the result of a singular polymorphic form or transition; rather, it arises from a spectrum of polymorphic transitions influenced by crystallization conditions and shown in Figure 2.

Polymorphic transitions in chocolate are inherently complex and dynamic, particularly in light of challenges such as fat bloom and the necessity of maintaining the stability of Form V. Achieving and confirming this specific polymorph is essential for proper tempering and overall quality. As discussed, polymorphism refers to the ability of a material to exist in more than one crystalline form. These different crystal structures can be characterized by features such as "short-spacing" and "long-spacing" arrangements—terms that describe the distinct distances between repeating units in the crystal lattice (short-spacing) or distances between lamella stacking (long-spacing). X-ray diffraction (XRD) is widely used to elucidate the crystal structures and more specifically wide-angle X-ray scattering (WAXS) has been used historically in CB research identification of specific polymorphisms. Today, WAXS in combination with differential scanning calorimetry (DSC) for determining of melting points are typically used to provide confirmation that Form V is the predominant polymorph in properly tempered chocolate. However, it should be noted that direct WAXS analysis of chocolate is complicated by the strong diffraction peaks of crystalline sucrose, which interfere with the detection of CB polymorphs. Consequently, either fat extraction or other sample preparation methods are often required when applying WAXS to finished chocolate products. Figure 3 illustrates typical WAXS patterns that highlights the short-spacing features alongside DSC thermogram curves for Forms IV, V, and VI. Historically, the use of such tools can be traced back to early observations of multiple melting points in tristearin (SSS),[23] although the underlying causes were not fully understood until further X-ray analysis was conducted by Clarkson and Malkin.[24] Since the 1930s, techniques such as WAXS, DSC, and polarized light microscopy (PLM) have been routinely employed to analyze melting profiles, polymorphic transitions, and crystal morphologies. While these methods are invaluable, they are not entirely unambiguous.[25]

Table 2. Short- and Long-Spacing of Cocoa Butter Polymorphs from Wide-Angle Powder X-ray Diffraction (WAXS) Data in the Literature[a]

	Literature			
polymorph	III (2L) B_2'	IV (2L) B_1'	V (3L) B_2	VI (3L) B_1
long-spacing (Å)	49	45	64.1	63.8
short-spacing (Å)	4.62 (w)	4.35 (vs)	5.4 (m)	5.43 (m)
	4.25 (vs)	4.15 (vs)	5.15 (w)	5.15 (w)
	3.86 (s)	3.97 (m)	4.58 (vs)	4.59 (vs)
	4.62 (w)	3.81 (m)	4.23 (vvw)	4.27 (vw)
			3.98 (s)	4.04 (w)
			3.87 (m)	3.86 (m)
			3.75 (m)	3.7 (s)
			3.67 (w)	3.36 (vw)
			3.39 (vw)	

[a]Data taken from ref 3. Letters in parentheses denote qualitative intensity, where "v" = very, "s" = strong, "m" = medium, "w" = weak, and combinations thereof.

Once it was recognized that Form V is strongly related to chocolate stability, researchers began to explore how other mechanical properties correlate with properly tempered chocolate. While WAXS has been instrumental in identifying the polymorphic forms of CB, complementary analytical techniques were developed to assess the texture and mechanical integrity of chocolate. For example, in the 1940s, the cone penetrometer was introduced to measure the consistency and yield value of plastic fats such as shortenings and margarines.[26] However, during this period, there were few instruments capable of gauging the hardness of food materials like chocolate. By the 1950s, the shore durometer became widely used for measuring the hardness of waxlike materials. This device, which features a frustoconical indentor driven by a spring and a scale-and-pointer mechanism to display the indentation depth, had its limitations—often reporting a value of 100 for hard samples, regardless of actual differences in hardness. Later, a modified Brinell test—originally developed for measuring the hardness of metals (ASTM method E 10−54 T)—was adapted for confectionary fats.[27] In 1942, Ravich and Volnova used this improved Brinell method to measure the hardness of tripalmitin and tristearin mixtures.[28] Rosenberg further refined this approach in 1954 to define the hardness of waxes.[29] Finally, in 1958, Lovegren, Guice, and Feuge introduced a method that provided a "hardness index" (in kilograms per square centimeter) for both tempered and untempered CB.[27] In addition to these methods, the three-point bending test, originally used for assessing the hardness and brittleness of ceramics and metals,[30] has become a standard for evaluating chocolate texture.[31−33] Modern texture analyzers, such as the TA XT Plus Texture Analyzer (Stable Micro Systems, Ltd., Scarsdale, NY, USA), perform high-precision three-point bending tests. In this test, a chocolate bar is supported on either side while a curved blade applies downward pressure at its center until it breaks (Figure 4) and calculated by use of eq 1.

$$E_e = \frac{Fa^3}{4dbh^3} \quad (1)$$

https://doi.org/10.1021/acs.cgd.5c00269
Cryst. Growth Des. 2025, 25, 2764−2783

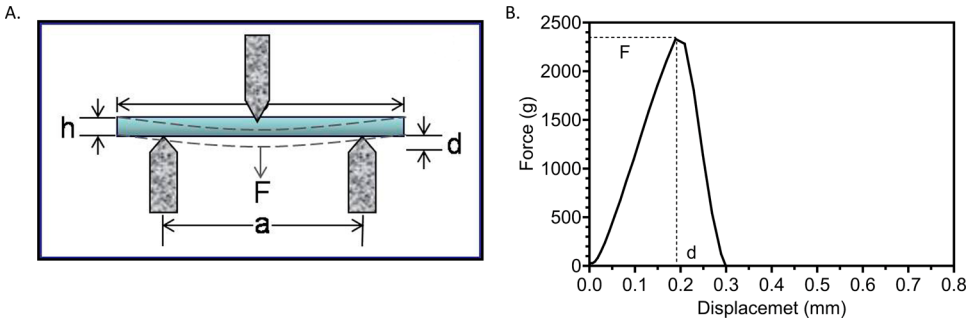

Figure 4. (A) Typical three-point bending setup and (B) typical corresponding force vs displacement profile.

where F is the applied force, a the span or distance between the two supports, d the midspan deflection or fracturability, b the sample width, and h the sample height.

In recent years, advancements in analytical techniques and mathematical modeling have provided deeper insights into polymorphism and bloom formation in chocolate. These include time-domain nuclear magnetic resonance (NMR) and DSC deconvolution for studying mixed CB polymorphism,[34] Raman spectroscopic methods (RSM) for evaluating fat crystallinity,[35] and Fourier transform infrared (FTIR) spectroscopy for analyzing polymorphic transitions in fats.[36] Atomic force microscopy (AFM) has been employed to investigate bloom development in chocolate,[37] while high-resolution and rapid data acquisition techniques such as synchrotron radiation X-ray diffraction have enhanced crystallization studies.[38] Additionally, terahertz spectroscopy has been utilized to examine CB crystallization,[39] and oil migration in chocolate has been explored through bloom development modeling by Green and Rousseau.[40] Furthermore, ultrasmall angle X-ray scattering (USAXS), combined with mathematical modeling, has been applied to study crystalline nanoplatelets (CNPs) and their aggregation behavior in various fat systems.[41] Regardless of these more-advanced techniques, the identification of Form V CB in chocolate by DSC thermal analysis and the short-spacing identification by WAXS is what is commonly accepted as the standard for chocolate quality.

THE EFFECT OF MINOR LIPIDIC COMPONENTS ON COCOA BUTTER CRYSTALLIZATION

Despite this established analytical framework, recent studies highlight the significant influence of processing conditions—such as temperature, pressure, and shear—on the kinetics of polymorphic transitions.[42] These variables can accelerate or delay transformations, impacting chocolate's microstructure and quality. Notably, research by Ghazani and Marangoni (2023) identified high-melting polymorphic forms of SSS and POS, illustrating how controlled crystallization environments yield novel crystalline phases with distinct properties.[7,43] Such transitions are particularly relevant to fat bloom, a major quality defect resulting from TAG migration, recrystallization, and polymorphic instability.[44] The role of minor lipids in crystallization and bloom formation is also critical; in 2000, Tietz and Hartel demonstrated that their removal slows nucleation, delays crystallization, and accelerates bloom formation.[45]

Since both internal (minor lipidic materials) and external (processing conditions) factors can influence the crystal structure, polymorphic transitions, and bloom development in chocolate, research has focused on the effects of minor lipidic materials in CB as seeding agents to eliminate the tempering process. These components can promote or inhibit CB crystallization parameters including nucleation, crystal growth, and polymorphic transition.[46] Research on the influence of minor components and additives on chocolate crystallization and bloom development has provided valuable insights. Early studies by Duck (1958 and 1963),[47,48] Kleinert (1961 and 1970),[16,49] Hettich (1964),[50] and Campbell and Keeney (1968)[51] reported the effects of increasing the apparent viscosity of molten dark chocolate and antibloom effects after the addition of chocolate powders as seed crystals during the tempering process.

Talbot, Smith, and Bhanggan showed that the amount of trisaturated TAGs and phospholipids in the CB seed crystals created at the beginning of crystallization was higher than their concentration in CB. They also found that free fatty acids (FFAs) can inhibit nucleation, while diacylglycerols (DAGs), particularly saturated DAGs, inhibit crystal growth—possibly by "poisoning" the crystal surface and preventing further molecular incorporation.[46] Following these realizations Tietz and Hartel removed the minor lipids from milk fat and then reintroduced them at twice their natural concentration. When this modified milk fat was added to CB at a 10% concentration, the result was longer nucleation times, slower crystallization, and faster bloom development compared to chocolate made with unmodified milk fat[45] while studies by Wright and Marangoni have found similar results.[52−54]

Similarly, Kinta and Hartel studied the effects of seeding on chocolate bloom, finding that seed quantity directly influences bloom development. Their work established that a concentration exceeding 270 ppm is required to form 2%−3% Form V crystals in chocolate, which, in turn, helps mitigate bloom.[22] Further advancing the understanding of seeding, in 1986, Hachiya, Koyano, and Sato examined how different seed crystals affect the kinetics of dark chocolate crystallization. They compared SOS in the β_1 form; a mix of pseudo-β' and β_2 polymorphs; 1,3-dibehenoyl-2-oleoylglycerol (BOB) in both β_2 and pseudo-β' forms; and SSS in the β form. Although all seed crystals enhanced crystallization, those with triacylglycerol compositions similar to CB were most effective. The observed order of effectiveness was: SOS (β1) > CB (Form V) > SOS (a mix of pseudo-β' and β_2) > BOB (β2) > BOB (pseudo-β') ≫ SSS (β).[55] In a subsequent study in 1990, Koyano, Hachiya, and Sato studied the effects of seeding to eliminate the tempering step of dark chocolate. In this study, they used CB (Form VI), SOS (β_1), BOB (pseudo-β'), BOB (β_2), and SSS (β). They showed all seeds caused an acceleration in the rate

https://doi.org/10.1021/acs.cgd.5c00269
Cryst. Growth Des. 2025, 25, 2764−2783

of crystallization. Bloom stability also was improved in dark chocolates containing all seeds except SSS in β polymorph.[56]

In addition to natural seeding and minor lipid studies, several researchers investigated the role of synthetic emulsifiers on bloom resistance. DuRoss and Knightly (1965) and Ludwig (1969) studied the effects of adding synthetic emulsifiers including sorbitan monostearate (Span 60), ethoxylated sorbitan monostearate (Tween 60), and polysorbate 60 to bloom resistance in tempered chocolate.[57,58] More recently, Aronhime and Garti[17] and Garti et al.[59] demonstrated that incorporating synthetic surfactants such as Tween 60 and Span 60 at concentrations of 1%−10% w/w can serve as effective antibloom agents in CB and chocolate. Together, these studies highlight the complex interplay between minor components, seeding agents, and synthetic emulsifiers in controlling chocolate crystallization and bloom development. While these approaches offer promising strategies for improving chocolate quality, attempts to use them to induce stable CB crystallization (Form V) and eliminate the tempering step entirely have seen limited success.

RECENT ADVANCES ON THE EFFECTS OF MINOR LIPIDIC COMPONENTS ON COCOA BUTTER CRYSTALLIZATION AND CHOCOLATE TEMPERING

Our recent work, including two key studies utilizing advanced X-ray and neutron scattering techniques, demonstrates that the Form V polymorph of CB alone does not dictate chocolate quality.[60,61] As extensively discussed, Form V is widely regarded as the ideal crystalline polymorph in chocolate due to its desirable texture and snap. However, our findings suggest that its presence does not necessarily prevent bloom formation. Instead, we determined that bloom formation is driven by microstructural defects, and one such factor is nonideal crystallite size and lattice strain.

We used small-angle X-ray scattering (SAXS) in our studies due to its ability to rapidly and unambiguously distinguish between Forms III, IV, and V based on a single characteristic diffraction peak, also known as the long-spacing reflection. This is in contrast to wide-angle X-ray scattering (WAXS)—more commonly known in the literature as powder diffraction—where phase identification requires multiple peaks, and peak overlap along with variations in intensity can complicate the differentiation of these polymorphs. Additionally, WAXS lacks the sensitivity to detect small quantities of minor polymorphic forms when a predominant form is present. By contrast, SAXS can detect trace amounts of Form IV in commercially tempered chocolates, underscoring its superior sensitivity in characterizing mixed polymorphic phases. It should be noted that Form VI has a similar long-spacing to Form V and when freshly tempered chocolate samples are used we presume no Form VI is present, and it is a caveat in this rapid identification. When Form VI is present, care must be taken to identify small shifts in long-spacing to lower values and a narrowed peak.

Although properly tempered samples primarily contain Form V, our data show that untempered samples exhibit significant variability, often containing a mixture of Forms IV and V, and at times, small amounts of Form III. The key findings of our studies emphasize that identifying microstructural defects—beyond just polymorphic form—is equally critical to chocolate stability. This insight underlines the importance of characterizing not only the polymorphic state of CB but also the underlying crystallite size and lattice strain, which we demonstrate can be effectively analyzed using a modified indexed Williamson−Hall (W−H) analysis.

In these key studies, we determined that by using a modified W−H analysis, one can leverage a SAXS pattern from chocolate to decouple the contributions of line broadening from crystallite size and microstrain of the CB within chocolate. The W−H analysis is a method used in diffraction studies to separate these two effects, allowing for a more comprehensive understanding of peak broadening mechanisms. This approach extends beyond the commonly used Scherrer equation (eq 2), which estimates domain (crystallite) size, D_p:

$$D_{\mathrm{p}} = \frac{K\lambda}{\beta \cos(\theta)} \tag{2}$$

where λ is the X-ray wavelength, β is the full-width-at-half-maximum (fwhm) of a reflection peak in units of radians, θ corresponds to the angular position of the center of the reflection peak, while K is a shape factor for the crystallite, usually assumed to be spherical and thus $K = 0.9$.

However, the fwhm of the peak is affected by several factors and not only crystallite size. Peak broadening can also arise due to lattice strain (and general disorder in the spatial distribution of atoms). So, without considering lattice strain, the crystallite size estimate using the Scherrer equation would be underestimated; it does not account for strain-induced broadening. In conventional diffraction analysis, peak broadening arises from two primary factors: (1) finite crystallite size and (2) lattice strain, both of which influence the diffraction pattern differently. The W−H analysis provides a means to distinguish these effects by incorporating both size and strain contributions into a single framework, and has begun to see applications in other fat systems such as margarines and oleogels.[62−64] The analysis is conducted by rearranging the Scherrer equation to solve for the line broadening term β (eq 3),

$$\beta = \frac{K\lambda}{D_{\mathrm{p}} \cos(\theta)} \tag{3}$$

as well as for microstrain (ε) (see eq 4),

$$\varepsilon = \frac{\beta}{4 \tan(\theta)} \tag{4}$$

The microstrain equation arises when the spacing between crystal planes (d) changes slightly, which, in turn, changes the Bragg angle (θ). Defining microstrain as $\varepsilon = \Delta d/d$, a small change in d results in a shift $\Delta\theta$ that can be approximated as $\Delta\theta \approx \tan\theta\, \varepsilon$. In practice, the peak width (β) measured as the fwhm reflects this shift. With some approximations and geometric considerations, the relation between the strain and the fwhm of the peak becomes eq 5. The factor of 4 specifically arises because we are using the fwhm in our analysis, rather than the integral breadth, which would use a factor of 2.[65,66]

$$\beta = 4\varepsilon \tan(\theta) \tag{5}$$

Recall that the total line broadening in diffraction data can then be described as the sum of contributions from microstrain and crystallite size (eq 6):

$$\beta_{\mathrm{total}} = \beta_{\varepsilon} + \beta_{D_p} \tag{6}$$

Thus, substituting eqs 3 and 5 into eq 6, we obtain

https://doi.org/10.1021/acs.cgd.5c00269
Cryst. Growth Des. 2025, 25, 2764−2783

$$\beta_{\text{total}} = 4\varepsilon \tan(\theta) + \frac{K\lambda}{D_p \cos(\theta)} \quad (7)$$

Expressing the lattice strain term tan θ by sin θ/cos θ, we obtain

$$\beta_{\text{total}} = 4\varepsilon \frac{\sin(\theta)}{\cos(\theta)} + \frac{K\lambda}{D_p \cos(\theta)} \quad (8)$$

Further rearrangement of eq 8 will result in the form used in the W−H plot,

$$\beta_{\text{total}} \cos(\theta) = \varepsilon 4 \sin(\theta) + \frac{K\lambda}{D_p} \quad (9)$$

A plot of $\beta \cos \theta$ on the y-axis, as a function of 4 sin θ on the x-axis, yields a linear regression with a slope and y-intercept that can be used to determine crystallite size and lattice strain (Figure 5). It should be emphasized that the lattice strain (ε),

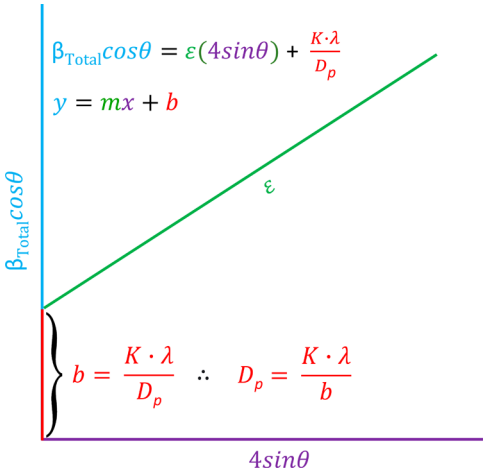

Figure 5. Visual representations of the W−H plot and the parameters one can derive from it, where the slope ε is equal to the lattice strain and y-intercept is used to solve for the crystallite size (D_p).

in our case, represents the distribution of the average lattice distortions or variations in the long-spacing (lamella thickness) of the Form V polymorph. This is expressed as a dimensionless value (i.e., $\Delta d/d$) as it quantifies the fractional deviation from the average lattice spacing. Traditional uses of the W−H method incorporate multiple reflections from different crystal planes in powder diffraction data. In chocolate samples, however, diffraction peaks from sugar interfere with the analysis because they dominate the XRD pattern at typical short spacings. In contrast, SAXS probes larger-scale structures and does not capture the diffraction peaks from sucrose crystals, making it a more suitable method for analyzing chocolate samples without additional sample preparation. The SAXS patterns of CB predominantly exhibited a reflection from the (001) crystal plane and its higher-order harmonics, (002) and (003). It should be noted that the designation of the (001) plane here follows the conventional usage in lamellar systems, describing the lamellar stacking direction rather than a crystallographic plane precisely indexed from the CB unit cell. Nevertheless, this lamellar reflection can still be treated as an indexed plane for the purposes of W−H analysis, which was used here to extract directional information on crystallite size and microstrain. This approach was used to evaluate the crystallite size and microstrain of CB crystals in chocolate tempered with phospholipids dimyristoylphophatidylcholine (DMPC) and dimyristoylphosphatidylethanolamine (DMPE), along with controls of tempered and untempered chocolates. This allowed for an anisotropic analysis focusing on the thickness of the lamellar domain in the Form V polymorph and microstrain, giving a new metric to chocolate bar analysis and quality beyond just identification on primarily Form V.

Summarizing the findings of our W−H analysis, we identified key metrics D_p and ε that can be used to evaluate whether a chocolate sample has been properly tempered. This metrics, summarized for 70% and 90% dark chocolates in Table 3, provides insight into the relationship between crystallite size and lattice strain in CB crystals.

Table 3. Crystallite Size and Microstrain for 70 and 90% Dark Chocolates[a]

sample	crystallite size, D_p (nm)	microstrain, ε
commercially tempered 70% chocolate	88.8	2.15
tempered 70% chocolate	89.5	2.94
untempered 70% chocolate	147	2.85
DMPE tempered 70% chocolate	96.8	2.82
commercially tempered 90% chocolate	75.4	3.10
untempered 90% chocolate	94.3	2.04
DMPC tempered 90% chocolate	129	6.93

[a]Data taken from refs 60 and 61.

Our analysis shows that, while the crystallite size of tempered chocolate CB varies, depending on the chocolate formulation—approximately 75 nm for a tempered 90% dark chocolate and ∼95 nm for tempered 70% dark chocolate—microstrain remains relatively constant across different formulations and should be targeted between 2.1ε and 3.1ε. This suggests that achieving both a sub-100-nm crystallite size and low strain is an essential indicator for properly tempered chocolate. It should be noted that the percentage value associated with a chocolate refers to the amount of cocoa solids present in the chocolate. These solids include cocoa mass (cocoa butter + cocoa powder) and added CB. The balance includes sugar and the emulsifier lecithin, used to help disperse sugar crystals in the CB phase. This is to say, the percentage of cocoa solids does not directly represent the amount of CB.

It is important to note that the values obtained from a W−H plot represent average estimates rather than absolute measurements, as they inherently reflect the overall characteristics of the sample rather than capturing localized variations in crystallite size and strain. Due to natural variability in crystal formation and distribution, these values should be interpreted as a relative gauge rather than exact targets. Comparing W−H data to a well-characterized control sample provides the most meaningful insights into chocolate tempering efficiency and structural integrity. Future research would benefit from a more comprehensive analysis of different chocolate formulations, including a broader range of CB concentrations from 50% to 100%, as well as milk chocolate and white chocolate. Expanding this approach to various formulations could provide a deeper understanding of how different fat compositions, emulsifiers, and nonfat solids influence crystallite size, strain, and overall chocolate stability and recommend targeted values for a tempered chocolate.

https://doi.org/10.1021/acs.cgd.5c00269
Cryst. Growth Des. 2025, 25, 2764−2783

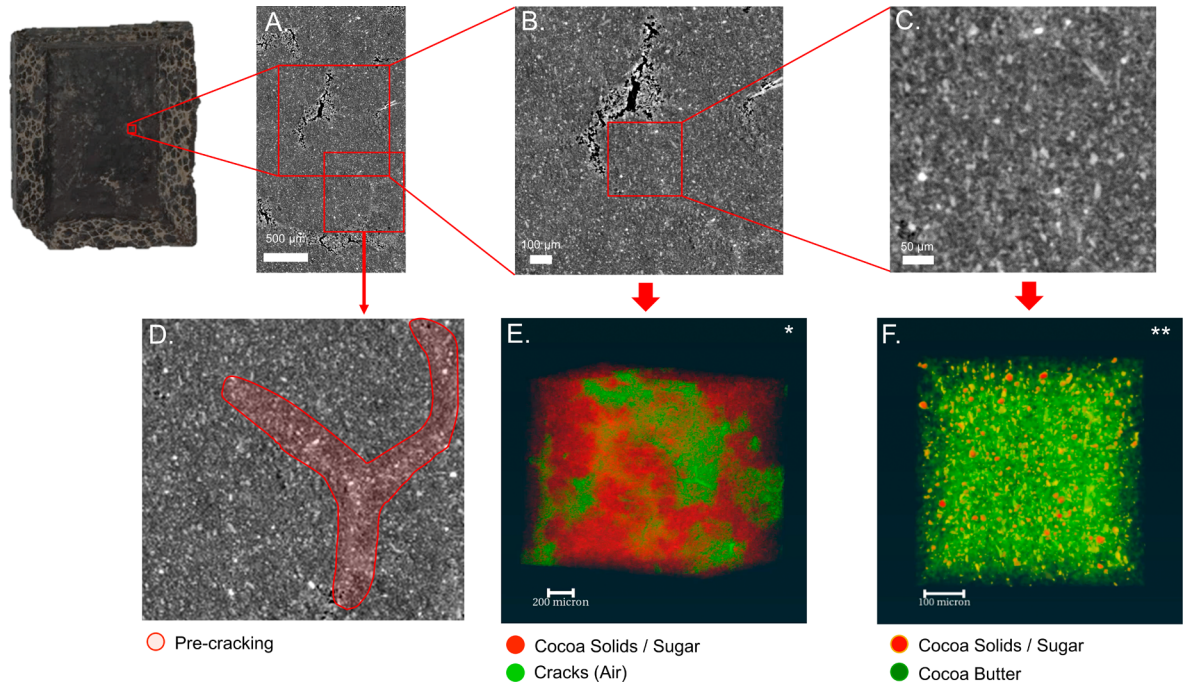

Figure 6. (A–C) Selected 2D SR-μCT slices comparing the macro- and microstructures of DMPC-tempered chocolate. Regions of precrack formation are highlighted in (D). (E) shows a low-magnification volume rendering of developed cracks (green), with cocoa solids and sugar in red and cocoa butter rendered transparent. In (F), a higher magnification of a similar region shows cocoa solids and sugar in yellow and red, and cocoa butter in green. [Schematic partially adapted from Chen et al.[32] and Stobbs et al.[60] Modified from the original by combining and adding panels.]

The Stobbs et al. studies also revealed the relevance of using synchrotron-radiation based microcomputed tomography (SR-μCT) phase contrast imaging (PCI) to analyze a larger size region between ~1 μm and 2000 μm. SR-μCT was used to investigate the effects of induced microstrain and uncontrolled crystal growth in chocolate samples, comparing commercially tempered chocolate with untempered samples, both with and without the added pure phospholipids DMPC and DMPE. This technique enables nondestructive three-dimensional imaging, allowing for the visualization and quantification of microscale structural defects such as air pockets and cracks. By applying phase retrieval methods,[67−69] an enhancement of the image contrast can be achieved compared to absorption based methods.[70−72]

In 2021, the Chen et al. study used this analysis and found that chocolate tempered with DMPC exhibited a microstructure similar to fresh commercially tempered chocolate at small length scales (below ~450 μm). However, in 2024, Stobbs et al. demonstrated that, at larger scales (~2 mm), significant defects, including cracks, were observed and can be seen in Figure 6. The commercially tempered chocolate displayed no major structural defects and consisted of a uniform mixture of cocoa solids, sugar, and CB, whereas the DMPC-tempered chocolate displayed noticeable cracks. Untempered chocolate exhibited even more substantial cracking. This technique allows for a 3D volume analysis to determine the fraction of cracks relative to total material volume. This study quantified these defects, showing that the volume fraction of cracks was 4.1% in the DMPC-tempered chocolate and 7.9% in the untempered chocolate. Additionally, the study revealed a phenomenon of "precracking", indicated by higher-density regions forming around developing cracks. This was detected in the DMPC-tempered and untempered chocolate samples but not in the commercially tempered chocolate and highlighted in Figure 6.

The study concluded that crack formation serves as a stress relief mechanism during uncontrolled CB crystal growth and is strongly correlated with bloom formation. The lower crack volume in DMPC tempered chocolate, combined with higher strain levels compared to untempered chocolate, indicates that DMPC tempered chocolate can endure greater stress without compromising mechanical properties. Despite expectations that higher strain might weaken the structure, the results suggest that DMPC-tempered chocolate retains mechanical properties similar to commercially tempered chocolate when DMPC is incorporated into the formulation.

In 2025, Stobbs et al. repeated the experiment with DMPE and analyzed multiple chocolate samples, including commercially tempered, hand-tempered, DMPC-tempered, DMPE-tempered, and untempered chocolate. The DMPC-tempered chocolate again exhibited extensive cracking, consistent with previous observations. In contrast, commercially tempered, hand-tempered, and DMPE-tempered chocolates showed no significant cracking or precracking, while the untempered chocolate displayed major defects. Noteworthy, they reported that handmade chocolate contained small air bubbles; however, these had no effect on cracking or bloom formation.

This later study also discussed an approach that goes beyond mere 3D visualization and quantification of cracking extent between samples. It introduced a qualitative volumetric analysis in which a histogram is produced from the 2D CT slices, representing the density distribution across the sample. Moreover, this approach—providing a rapid method for interpreting structural differences—differs from histograms derived from segmented data (e.g., particle size distributions obtained from time-consuming 3D segmentations). Analyzing this histogram enables comparisons between scans and reveals

https://doi.org/10.1021/acs.cgd.5c00269
Cryst. Growth Des. 2025, 25, 2764−2783

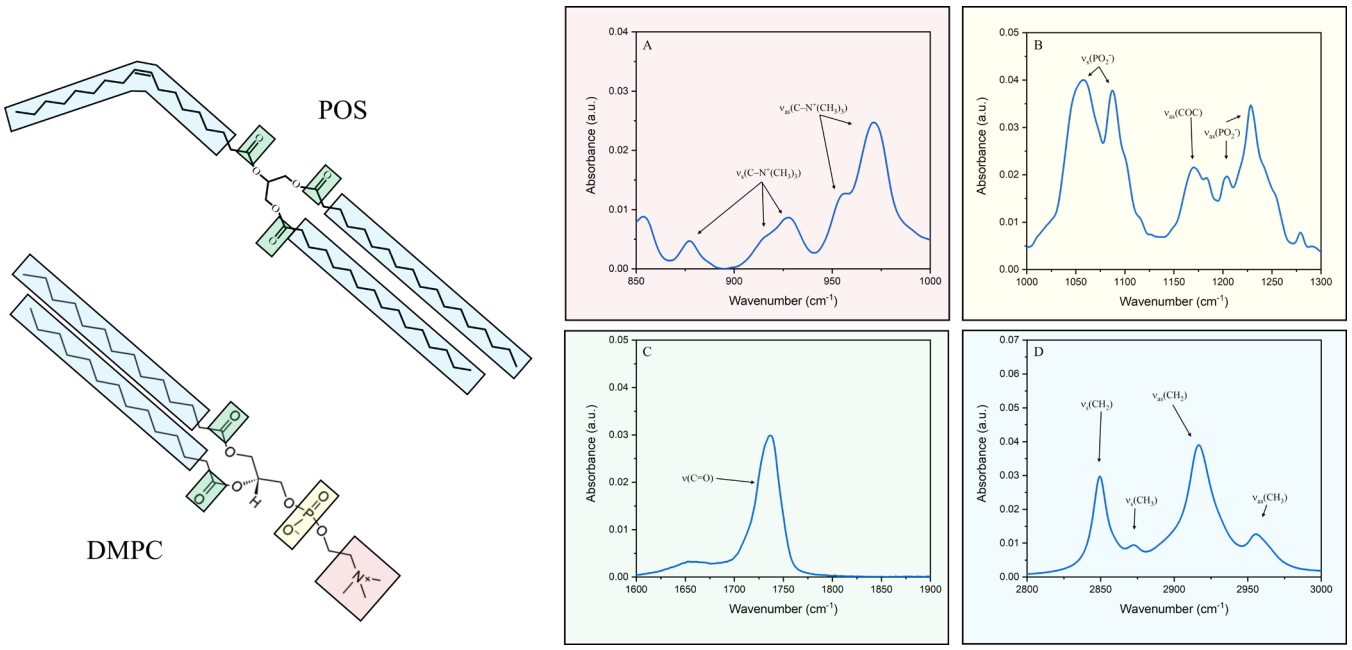

Figure 7. Molecular structure of DMPC and POS with color-coded functional groups corresponding to the displayed FTIR spectra of (A) choline moieties, asymmetric C−N stretch ($\nu_{as}C-N^{+}(CH_3)_3$) and symmetric stretching of $-N-(CH_3)_3$ and asymmetric C−H bending of polar headgroup in DMPC (red); (B) phosphate moieties of asymmetric ($\nu_{as}(PO_2^{-})$), symmetric ($\nu_s(PO_2^{-})$) in DMPC (yellow); (C) ester moieties of C═O in both DMPC and POS (green); and (D) alkyl chain moieties of symmetric and asymmetric $\nu_s(CH_3)$, $\nu_{as}(CH_3)$, $\nu_s(CH_2)$, and $\nu_{as}(CH_2)$ in DMPC and POS (blue). [IR spectra in the schematic were partially adapted from Stobbs et al.[60] Modified from the original by isolating the DMPC spectrum and adding color-coded regions corresponding to the functional groups of the DMPC/POS molecule.]

variations in volumetric density across samples. Structural differences lead to distinct peaks at various gray values, with lower-density materials generally appearing at lower gray values compared to higher-density materials. For example, in chocolate, air bubbles appear darker and form a peak at the lowest gray values, while CB appears slightly brighter, followed by sugar and cocoa solids. When these histograms are normalized for volume, the peak height—or the integral of the peak—represents the total volume of the corresponding material. Although exact gray values may vary with the experimental setup and reconstruction parameters—especially in phase-retrieved CT data, where phase fringes at material interfaces can shift the peak positions—relative comparisons of peak positions, widths, and heights enable conclusions about average particle or pore distributions between samples. For instance, when air bubbles become smaller, the corresponding dark peak shifts downward, and a widening of the peak indicates a broader size distribution, and vice versa. This histogram analysis approach has been reported on increasingly in cases of soft material analysis.[70,73−75] Stobbs et al. used this technique to attribute the wider density distribution observed in commercially tempered and DMPE-tempered chocolates, compared to untempered or DMPC-tempered chocolates to a more homogeneous material, serving as a valuable indicator for proper tempering via SR-μCT.

A key takeaway from this study, not extensively emphasized, is the advantage of SR-μCT's nondestructive imaging and extreme sensitivity via phase contrast. This capability allows for the detection of microscale defects but, more importantly, the identification of precracking before a crack fully develops. The ability to detect higher-density regions in precracking stages, as observed in DMPC-tempered and untempered samples, suggests that this technique could be applied to investigate chocolate confections while still in their packaging. Such early detection could serve as a valuable quality control tool, enabling manufacturers to assess potential structural issues before visible defects form. This would allow for quicker corrective actions in formulation and manufacturing, reducing product waste and improving consistency.

These two studies revealed that the phospholipids DMPC and DMPE both "temper" chocolate by promoting primarily Form V polymorphism. However, they do so via different mechanisms, with nucleation dynamics playing a far more influential role than achieving Form V polymorphism alone. This observation highlights another interesting aspect of these studies—the application of mid-IR spectroscopy to observe molecular-scale interactions and the chemical environment. Although mid-IR is a mature technique, it fills an important gap in our developing multiscale framework. We will not delve into its theory and applications as extensively as with SAXS and SR-μCT, but we will underscore its importance in confirming some of our claims.

There are two main IR regions that overlap in the mid-IR for phospholipids and TAGs: the ester C═O moieties between 1720 and 1760 cm^{-1} and the alkyl chain region between 2800 and 3000 cm^{-1}, which corresponds to CH_2/CH_3 vibrations. The ester carbonyl peaks can be used to observe shifts and changes in shoulder features; however, due to the overlapping contributions from phospholipids and TAGs, these peaks can only be interpreted as indicating changes in the overall hydrogen bonding of the system—not solely that of the phospholipid or TAG component. The alkyl chain region is analyzed similarly, but by using deuterated phospholipids, one can separate the contributions of TAGs from those of the phospholipids. When a deuterated phospholipid is used, the CD_2/CD_3 peaks shift to the 2150−2250 cm^{-1} region, allowing changes in the chemical environment of the alkyl chains of TAGs and phospholipids to be attributed separately.

https://doi.org/10.1021/acs.cgd.5c00269
Cryst. Growth Des. 2025, 25, 2764−2783

Phospholipids also contain a polar headgroup. For example, DMPC has a choline headgroup that exhibits specific and well-known vibrational modes from C−N stretching in its solid, micellar, and dissolved/dispersed forms, appearing between 850 and 1000 cm^{-1}.[76] One can analyze peak shifts or broadening in this region to assess changes in polarity and the disorganization of highly ordered crystalline states. Additionally, phospholipids contain a phosphate group with vibrational modes between 1000 and 1300 cm^{-1}, which can provide information on the hydrogen bonding between adjacent DMPC molecules.

These key vibrational modes are highlighted for a POS and DMPC molecule in Figure 7. Our studies applied mid-IR analysis of DMPC/DMPE and POS interactions to support our claims of significantly different mechanisms for Form V CB production with phospholipids—namely, micellar aggregation in the case of DMPC-POS and macroscale nucleation via particle integration for DMPE-POS. In summary, the ATR-FTIR data demonstrate that the interaction of DMPC with POS primarily disrupts the hydrogen bonding and organization of its polar head groups while leaving the nonpolar alkyl chains unchanged. The use of deuterated phospholipids effectively decouples these contributions, allowing us to clearly attribute the observed spectral shifts to modifications in the polar moieties rather than the TAG (alkyl chain) components. Furthermore, IR analysis supports a mechanism in which DMPE acts primarily as a physical nucleation surface rather than engaging in strong molecular interactions with POS. The IR data reveal that DMPE exhibits only limited interactions with POS, in contrast to DMPC. This limited interaction confirms that DMPE remains solid under typical processing conditions due to its high melting point and low solubility in CB. Consequently, when DMPE is mechanically fragmented or solvent-mediated dissolution to increase its surface area, it provides stable nucleation sites for Form V CB crystals without inducing lattice strain or defects. This study demonstrated importance of IR spectroscopy for characterizing molecular interactions between phospholipids and TAGs, offering critical insights into nucleation dynamics and hydrogen bonding in these systems.

A final key technique worth mentioning in these studies was the use of environmental scanning electron microscopy (ESEM), which provided insights into the microstructure of the solid-state phospholipids. As shown in Figure 8, ESEM

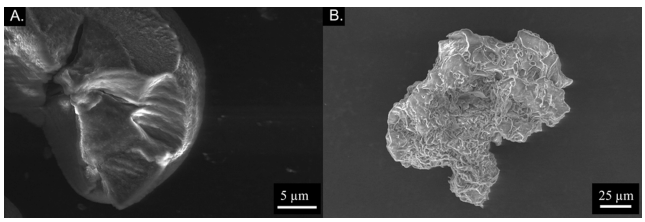

Figure 8. Environmental scanning electron microscopy of (A) ground DMPE and (B) DMPC. [Adapted from Stobbs et al. (2025).[61]]

images reveal a clear distinction between ground DMPE (Figure 8A) and DMPC (Figure 8B). Unlike DMPC, which, upon dissolution, forms micelles that introduce lattice strain and defects, DMPE does not self-assemble into such structures. Instead, DMPE serves as a solid-state nucleation surface that guides CB into the stable Form V polymorph without compromising microstructural integrity.

However, while DMPE demonstrates that controlled nucleation can stabilize chocolate microstructure, it also raises a critical question: If Form V CB is the key to chocolate stability, why does bloom still occur in samples that predominantly exhibit Form V? Traditional wisdom suggests that once chocolate reaches Form V, it should remain stable; yet, numerous studies—including our own—have found that Form V alone does not guarantee long-term structural integrity.

We have extensively discussed that traditional tempering protocols have long been considered essential for directing CB crystallization. Yet, our findings reveal that stable CB crystals can form with minimal temperature cycling—without the need for shear—when specific molecular interactions are introduced during early crystallization stages. In essence, chocolate crystallization is a multiscale phenomenon that spans from molecular interactions and initial nucleation, through supramolecular and nanoscale ordering to microscale structuring. This underscores the importance of crystal history—how crystals form, not just their final polymorphic state.

In summary, our advanced characterization techniques and targeted nucleation strategies highlight the complex, multiscale nature of chocolate crystallization. From early nucleation events to the development of stable microstructures, our findings emphasize that both the formation pathway and final polymorphic state are critical for achieving high-quality, bloom-resistant chocolate.

To further emphasize this, we turn to new experimental data that highlights cases where Form V polymorphism is present, yet bloom and microstructural differences develop. Notably, even among samples exhibiting Form V, variations in structure at different length scales are evident, indicating that factors beyond the final polymorphic state contribute to chocolate stability.

BEYOND POLYMORPHISM: INSTABILITY IN CB WITH FORM V

Chocolate samples were produced identically to Stobbs et al. 2025 and stored for 1 year at 18 °C to further demonstrate that achieving Form V polymorphism does not inherently ensure stability. To accomplish this, we present images of four chocolate samples with varying tempering conditions: (A) untempered, (B) DMPC-tempered, (C) DMPE-tempered, and (D) tempered chocolate (Figure 9).

The untempered chocolate (Figure 9A) serves as a clear baseline for instability, exhibiting extensive fat bloom and structural imperfections due to uncontrolled crystallization. This is expected, as the absence of tempering results in a disordered crystal network with unstable polymorphic forms. The DMPC tempered chocolate is particularly revealing. Despite being confirmed primarily as Form V by SAXS,[60] and seen in Figure 10, it exhibits pronounced fat bloom.

This directly challenges the long-held assumption that achieving Form V guarantees long-term stability. These results also show that the chocolate did contain small amounts of Form IV and therefore can be argued would bloom. Recall Stobbs et al. (2025) repeated the experiments with DMPE.[61] Comparison of a commercial with a hand-tempered chocolate, revealed that small amounts of Form IV were present in both, but did not readily bloom. This finding supports the notion that the presence of small amounts of Form IV cannot solely be responsible for the bloom effect, or else one would expect bloom to be observed in these samples as well. Stobbs et al.[60]

https://doi.org/10.1021/acs.cgd.5c00269
Cryst. Growth Des. 2025, 25, 2764−2783

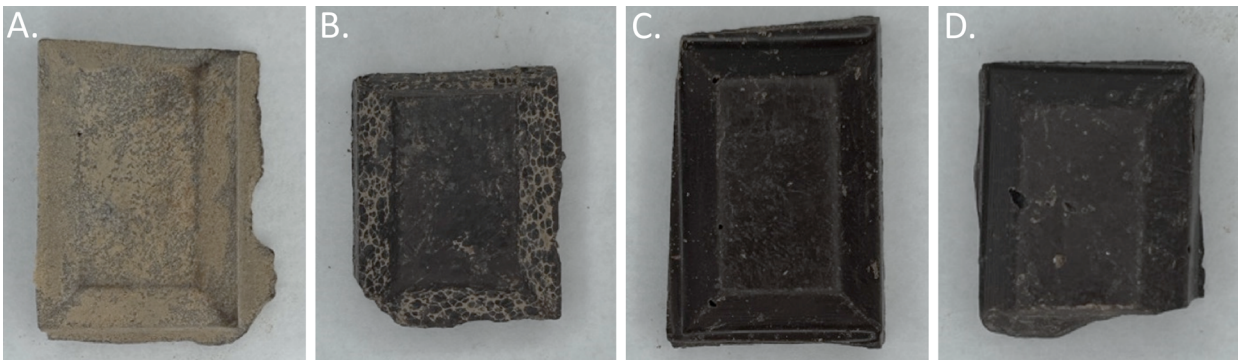

Figure 9. Images of chocolate produced and stored for 1 year at 20 °C to observe bloom formation: (A) untempered, (B) DMPC-tempered, (C) DMPE-tempered, and (D) tempered. All chocolate other than the DMPE-tempered formed varying levels of bloom during the storage period.

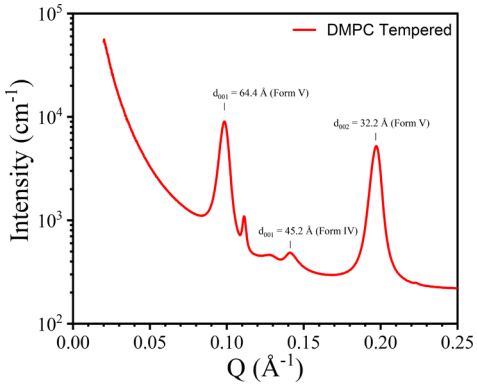

Figure 10. Small-angle X-ray scattering pattern of DMPC-tempered chocolate shown to be primarily in Form V with small amount of Form IV CB. [Modified image from Stobbs et al.[60] by replotting data with only the DMPC SAXS pattern.]

proposed a possible explanation for this observation of bloom in DMPC-tempered samples. They suggested that DMPC forms micelles in molten CB, introducing lattice strain during crystallization and combined with the formation of large crystallites after crystallites had a nonideal nanomicrostructure that was prone to bloom formation.

Next, we show an example highlighting an interesting case where polymorphism seems to be disconnected from structural integrity of a chocolate. We conducted a three-point bending analysis that evaluates a chocolate's structural integrity by quantifying its bending elastic modulus (N/mm^2), which reflects the material's resistance to deformation under stress. Properly tempered high-quality dark chocolate is expected to be firm and produce a strong snap upon breaking, in contrast to under-tempered samples. We supply a WAXS analysis confirming the presence of the desired Form V polymorph in both tempered and untempered chocolate (Table 4) and on the same samples our results demonstrate that tempered chocolate exhibited a bending elastic modulus of 427 N/mm^2, whereas untempered chocolate had a significantly lower value of 97.6 N/mm^2 (Figure 11). This large difference indicates that while both chocolates are primarily in the Form V polymorph, their mechanical properties differ substantially, due to variations in microstructure. The higher modulus in tempered chocolate reflects a more rigid and cohesive fat crystal network, which is essential for achieving the characteristic texture and snap. Conversely, the lower modulus in untempered chocolate suggests a weaker, more deformable structure.

This is a clear example where WAXS fails to capture the subtle differences in mechanical properties among samples sharing the same polymorphic form, potentially leading to the misclassification of an untempered sample as tempered.

A final note to address, it is important to recognize that even combining WAXS analysis with mechanical testing does not provide a definitive assessment of tempering quality. Chen et al.[32] reported that chocolate tempered with DMPC matched conventional tempered chocolate in both polymorphism and elastic bending modulus. However, as Stobbs et al.[60] showed, significant differences in microstructural properties were still present and resulted in bloom formation, highlighting the necessity of determining microstrain and crystallite size in tempering evaluations or analysis of chocolates.

Table 4. Literature Values of XRD Short Spacings of Known CB Polymorphs (Forms III−VI)[a]

	literature[b]					Sample	
	polymorph III (2L) B_2'	polymorph IV (2L) B_1'	polymorph V (3L) B_2	polymorph VI (3L) B_1	peak #	tempered	untempered
short spacings (Å)	4.62 (w)	4.35 (vs)	5.4 (m)	5.43 (m)	1	5.4 (m)	5.4 (m)
	4.25 (vs)	4.15 (vs)	5.15 (w)	5.15 (w)	2	5.20 (w)	5.23 (w)
	3.86 (s)	3.97 (m)	4.58 (vs)	4.59 (vs)	3	4.57 (vs)	4.59 (vs)
	4.62 (w)	3.81 (m)	4.23 (vvw)	4.27 (vw)		–	–
			3.98 (s)	4.04 (w)	4	3.97 (s)	3.99 (s)
			3.87 (m)	3.86 (m)	5	3.85 (m)	3.89 (m)
			3.75 (m)	3.7 (s)	6	3.74 (m)	3.76 (m)
			3.67 (w)	3.36 (vw)	7	3.65 (w)	3.68 (w)

[a]Tempered and untempered chocolate samples are shown to have the same polymorphism (Form V). Letters in parentheses denote qualitative intensity, where "v" = very, "s" = strong, "m" = medium, "w" = weak, and combinations thereof. [b]Data taken from ref 3.

https://doi.org/10.1021/acs.cgd.5c00269
Cryst. Growth Des. 2025, 25, 2764−2783

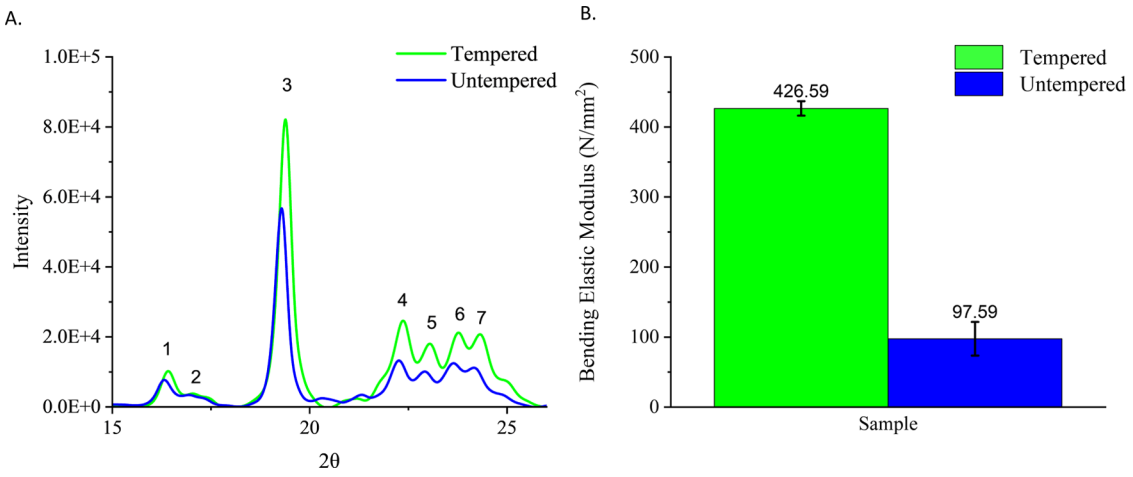

Figure 11. (A) XRD patterns of tempered and untempered dark chocolate showing that the cocoa butter crystals in both chocolates are in Form V, regardless of the tempering. Peaks 1−7 are the shorting spacings of the Form V polymorph at 5.4, 5.21, 4.57, 3.97, 3.85, 3.74, and 3.65 Å. B) Elastic bending modulus of tempered and untempered chocolate. A higher modulus is correlated with better snap (brittle fracture).

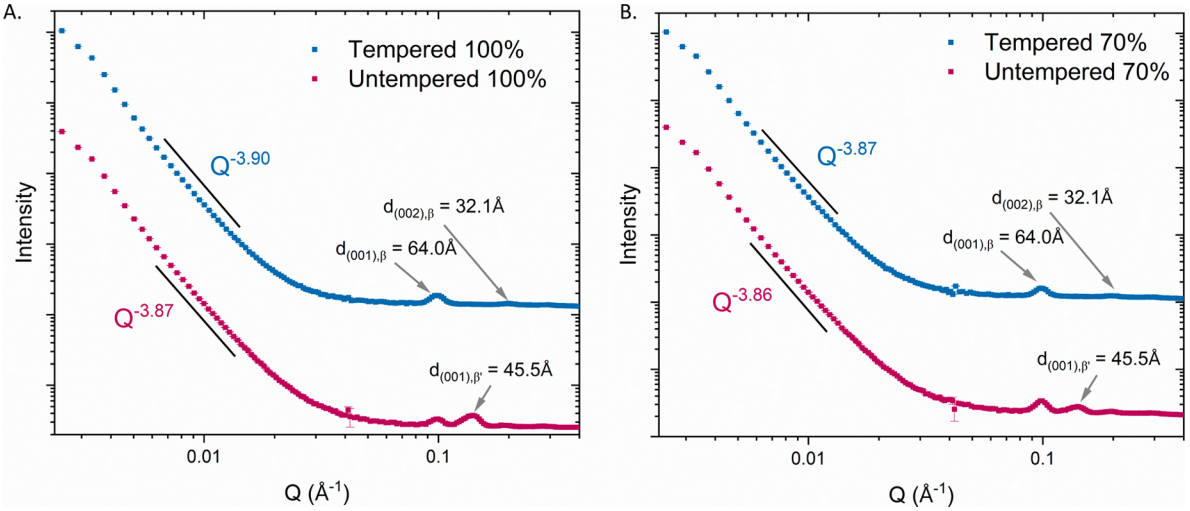

Figure 12. Small-angle neutron scattering (SANS) profiles of tempered and untempered 100% (A) and 70% (B) dark chocolates. Due to background scattering contributions from sugar and cocoa solids, the decay exponents are similar and no significant differences can be observed.

As previously discussed, using SAXS provided additional structural indicators beyond polymorph identification, offering new parameters for assessing proper tempering. Specifically, a modified W−H analysis allowed us to examine both micro-strain and crystallite size.

While those studies highlight the potential of alternative nucleation enhancement strategies, the key takeaway remains: Form V polymorphism is not a guarantee of stability. These findings further suggest a need to reconsider the role of polymorphism in chocolate tempering and shift focus toward a more comprehensive understanding of crystallization dynamics through multilength scale lenses from nanocrystallite size, strain, and structures.

Many of the same analysis techniques described above by using SAXS can be used on small-angle neutron scattering (SANS) data. We conducted SANS experiments on tempered and untempered CB samples, which is another technique for probing supramolecular nanolength scales.

It should be noted that when SANS/SAXS is applied to chocolate samples, scattering from cocoa solids and sugars introduces a background level comparable to that from pure CB, which affects the information extracted from both the Guinier and Porod regions. The Guinier region is the low-Q region, typically defined by the condition $Q{\cdot}R_g \lesssim 1{-}1.3$ (where R_g is the radius of gyration). In this regime, the scattering intensity decays exponentially, according to eq 10:

$$I(Q) \approx I(0)^{(-Q^2 R_g^{\,2}/3)} \tag{10}$$

Analysis in this region yields the overall size (or radius of gyration) of the scattering entities and is sensitive to their bulk or average dimensions. Although the precise Q range depends on the sample, it is often observed near Q values of ∼0.01 Å^{-1}. The Porod region is the high-Q region where the intensity decays following a power law, typically close to eq 11:

$$I(Q) \propto Q^4 \tag{11}$$

This decay is characteristic of systems with sharp interfaces and provides information on the surface area and interface sharpness or roughness of the scattering objects. Deviations from the ideal Q^{-4} behavior can indicate the presence of fractal structures or diffuse interfaces. For many samples, the analysis of the Porod region typically occurs between Q values of ∼0.03−0.05 Å^{-1}. Thus, while the Guinier region is used to

https://doi.org/10.1021/acs.cgd.5c00269
Cryst. Growth Des. 2025, 25, 2764−2783

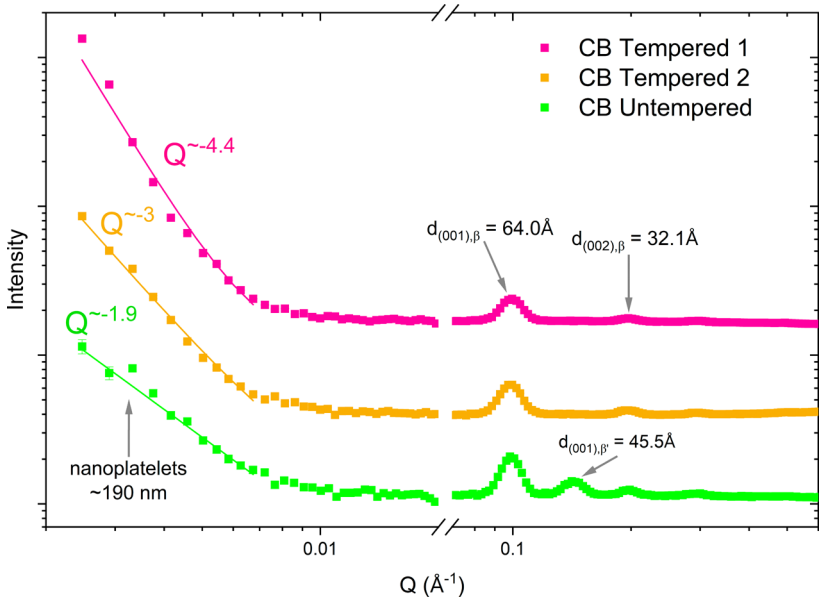

Figure 13. Small-angle neutron scattering (SANS) profiles of two tempered CB (pink and tan) and untempered CB (green). All samples display the Form V diffraction peaks at 64.0 Å and 32.1 Å, while only the untempered sample displays a diffraction peak of Form IV at 45.5 Å, and an additional peak at ∼190 nm, possible from CNP. Slope exponents are displayed for each sample.

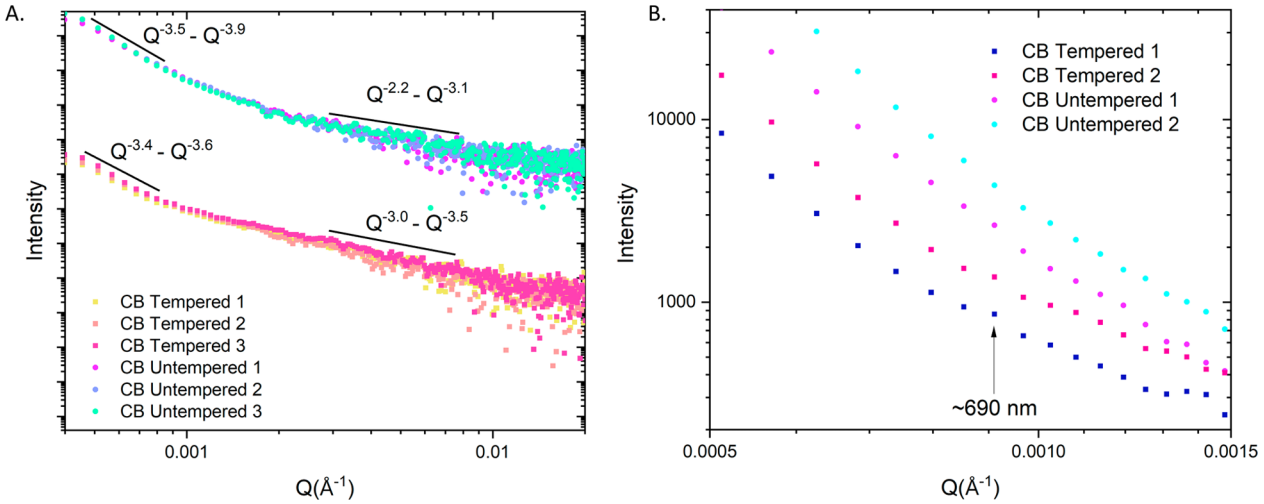

Figure 14. (A) Ultra-small-angle X-ray scattering (USAXS) profiles of tempered and untempered CB showing two distinct regions which can be analyzed. (B) Lower Q values of selected samples, highlighting a structural feature with periodic order at ∼690 nm.

extract the overall size of the scattering particles, the Porod region offers insights into surface characteristics and internal structure sharpness.

Analyzing chocolate samples is challenging because sugar and cocoa solids alter the scattering decay laws. Figure 12 shows that both tempered and untempered 100% chocolate (Figure 12A) and 70% chocolate (Figure 12B) yield nearly identical power-law slopes (−3.86 to −3.90). Decoupling the contributions from cocoa solids, sugar, and CB may be possible, but it requires further investigation and should be a focus for developing industry-relevant analytical techniques that address analysis at these specific length scales, making background subtraction a critical aspect of this work.

In Figure 13 we show three samples of CB: two tempered and one untempered. As expected, we observed the Form V polymorph in all samples by identifying the long spacing reflections from the (001) and (002) crystal planes at 64.0 Å and 32.1 Å, respectively. Additionally, in the untempered sample, we detected a reflection at 45.5 Å, corresponding to the (001) plane of Form IV in a 2L configuration.

It is also notable that the untempered chocolate exhibits a peak at approximately 190 nm, which may correspond to ordered nanoplatelets known to exist in pure fats.[77,78] These structures become less apparent or disappear in the tempered samples, likely due to a broader size distribution and the smoothing of grain-boundary interfaces during the tempering process. This suggests that tempering not only influences polymorphic transformation but also affects the nanostructural and mesoscale organization of fat crystals.

When fitting a power-law decay function to the scattering profiles, we observe that the intensity decays proportional to $Q^{-1.9}$ for the untempered sample and $Q^{-4.4}$ and $Q^{-3.0}$ for the tempered samples. The untempered sample, with an exponent of ∼1.9, suggests a more open and porous microstructure,

https://doi.org/10.1021/acs.cgd.5c00269
Cryst. Growth Des. 2025, 25, 2764−2783

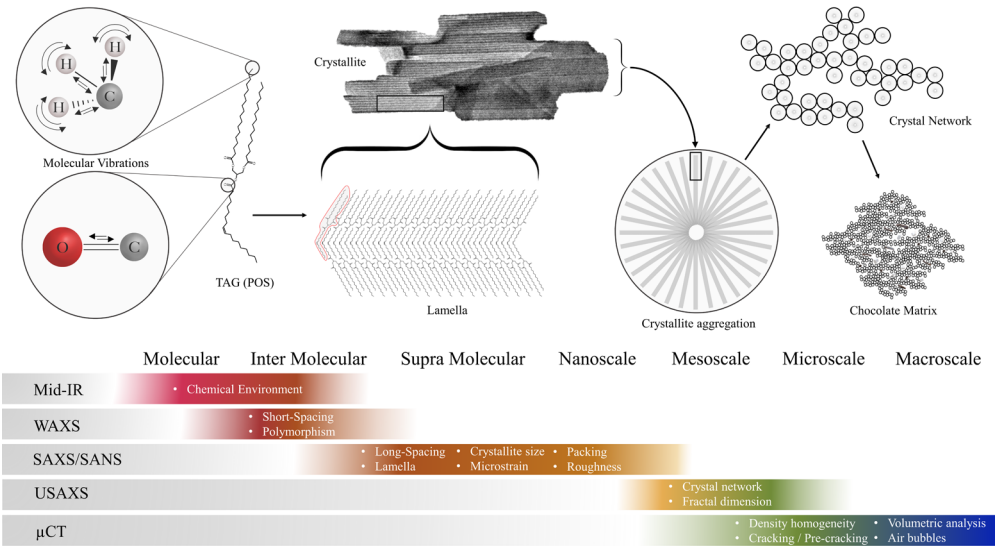

Figure 15. Visual schematic of the multiscale fat crystallization process observed by Mid-IR, WAXS, SAXS/WAXS, USAXS, and μCT.

indicative of a loosely packed, less-ordered fat crystal network, probably corresponding to a mass fractal.[79] The tempered sample with an exponent of ∼4.4 suggests the presence of sharp interfaces and well-defined crystalline structures, indicative of a smooth, compact morphology with minimal surface roughness in the size range of hundreds of nanometers, probably corresponding to a surface fractal.[79] In contrast, the tempered sample with an exponent of ∼3 exhibits characteristics of a Euclidean mass fractal structure. A mass fractal can have dimensionalities (D_m) between 1 and 3. A D_m value of 1 would indicate a linear aggregate while a D_m value of 3 is indicative of a Euclidean object, such as a sphere, implying a more diffuse or partially aggregated organization at this nanoscale range.[80]

This difference between the tempered samples further underscores the importance of microstructural analysis. While both samples exhibit Form V polymorphs, their differing microstructures highlight how subtle variations in crystallization history can significantly impact the final fat organization. An ideal structural target would be an exponent approaching −4, indicative of a highly compact and uniform crystal network. This analysis again reinforces the need to consider structural organization beyond simple polymorphic identification, emphasizing how processing conditions directly influence the final properties of chocolate; however, further studies need to be done to confirm that a proper tempered chocolate with no blooming does have exponent of −4.

So far, we have discussed techniques that examine different length scales: μCT covers structures from millimeters down to micrometers, SAXS/SANS probe approximately 1 to 200 nm, and WAXS investigates atomic distances from about 1 Å up to 10 nm, and IR covers molecular scale interactions. However, there remains a critical gap in the mesostructural range, roughly between ∼200 nm and 1 μm. To fill this gap, ultra-small-angle X-ray scattering (USAXS) and ultra-small-angle neutron scattering (USANS) can be employed. Here, we will only discuss USAXS, although USANS can be applied similarly.

In the USAXS regime, this size range provides insight into CNP lengths and their aggregation into larger structural features. Figure 14A presents data from both tempered and untempered samples, revealing variations in power-law regions. At lower Q values—between approximately 0.001 and 0.0001 Å^{-1}, both samples exhibit similar slopes, between 3.5 and 3.9. This region primarily reveals information about the overall size and shape of the CB crystallites, capturing larger-scale, submicrometer features while also reflecting the degree of surface roughness or fractal character (a perfectly smooth interface would yield a slope of − 4). Although the overall behavior is similar, untempered CB appears to have a higher variance in roughness compared to tempered CB. At higher Q values—ranging from ∼0.01 to ∼0.09 Å^{-1}—the slopes diverge significantly. Tempered chocolate shows slopes of −3.0 to −3.5, indicating that the interfaces are relatively more defined and homogeneous, and possibly correspond to a surface fractal. In contrast, untempered CB exhibits slopes between −2.2 and −3.1, suggesting a mass-fractal structure with a higher degree of roughness or diffuse interfaces, indicative of more heterogeneity in the mesoscale crystal structure. In summary, the lower-Q region probes larger-scale features, such as the overall dimensions and general interface characteristics of the CB crystallites, while the higher-Q region focuses on finer, nanometer-scale details, including the sharpness and fractal nature of the interfaces.

At higher Q values (around Q = 0.1 Å^{-1}), Figure 14B reveals a subtle yet distinct diffraction peak in tempered CB, corresponding to a high degree of regularity with a characteristic length of approximately 690 nm—likely reflecting the average length of a CNP or CNP multimer.[77] The presence of this peak in tempered CB, but not in untempered CB, likely arises from the shear forces during tempering, which promote a narrow size distribution and preferential alignment of the crystals. Untempered CB, with its broader variability in size and orientation, does not develop this degree of periodic order, and thus the peak is absent.

These findings suggest that, when analyzing CB via USAXS some key target values include low-Q slopes of −3.5 to −3.9 for overall crystallite dimensions and interfacial roughness, high-Q slopes of −3.0 to −3.5 for tempered CB and −2.2 to −3.1 for untempered CB, highlighting differences in the grain-boundary interface; however, further studies to determine which range of key target values result in well-tempered chocolate that do not bloom need to be undertaken. A diffraction peak at $Q \approx 0.001$ Å^{-1} with a characteristic length

https://doi.org/10.1021/acs.cgd.5c00269
Cryst. Growth Des. 2025, 25, 2764−2783

of ∼690 nm as an indicator of periodic order in tempered samples. It is important to note that these values are subject to experimental uncertainties and sample variability. Although our USAXS analysis focused on CB and did not include chocolate samples, the same challenges—namely, the overlapping contributions from cocoa solids and sugar—apply when analyzing chocolate. Future investigations should address whether these contributions can be effectively decoupled, as suggested by SAXS results, and validate these findings across a broader range of samples.

REDEFINING THE DOGMA OF CHOCOLATE TEMPERING

This Perspective has revealed that Form V alone does not define proper chocolate tempering. Instead, chocolate stability emerges from a multiscale phenomenon governed by nucleation dynamics, molecular organization, and both physical and chemical lipid interactions. In other words, the history of crystallization—the pathway to the final structure—is as crucial as the end point. This comprehensive view explains why bloom may occur, even when Form V is present.

By shifting focus from rigid, single-marker classifications, such as those based solely on polymorphism or traditional XRD/WAXS and DSC methods, we propose a refined evaluation of chocolate quality. Emphasizing a multiscale framework not only deepens our understanding of tempering but also unlocks new strategies to optimize nucleation dynamics, reduce energy costs, simplify processing, and ultimately enhance product quality.

Our framework redefines chocolate tempering by integrating a suite of analytical techniques that probe different length scales—from molecular interactions to macroscopic structures and show in Figure 15. By coupling these methods, we have a more intricate understanding of tempering but also define specific metrics that underpin long-term stability in properly tempered chocolate and we will summarize below.

At the molecular scale, IR spectroscopy is central to detecting subtle changes in chemical bonds and molecular interactions within the lipid matrix. IR can monitor shifts in vibrational modes associated with hydrogen bonding, which, in turn, reflect alterations in fatty acid chains and packing. For instance, by focusing on the alkyl chains and ester moieties in both major and minor lipid components, IR spectroscopy provides insight into the order or disorder of the molecular arrangement. Although these techniques have long been used in analyzing CB behavior, they remain critical for understanding how additives or processing conditions influence early crystallization dynamics.

Complementing IR, WAXS offers detailed insights into the crystalline structure of cocoa butter. WAXS is particularly adept at resolving characteristic distances between atomic planes in crystals, a key marker for identifying the Form V polymorph traditionally associated with proper tempering. However, while WAXS effectively distinguishes major polymorphic forms, it can suffer from lack of sensitivity and possibly resolution to detect the presence of minor phases, such as small amounts of Form IV or VI in the presence of a predominantly Form V polymorph. Its reliance on multiple peak assignments also makes it less robust and efficient when compared to scattering techniques that only require a single peak polymorphic determination.

Moving to the nanoscale and supramolecular organization, SAXS and SANS provide complementary information about the chocolate fat matrix. SAXS is uniquely suited to measuring the long-spacing lamella thickness—typically around 6.4 nm in a well-tempered sample—and supports the use of the indexed W−H analysis to quantify ideal microstrain and crystallite size. In practice, SAXS reveals crystallite dimensions on the order of ∼100 nm and microstrain values in the range of 2.1−3.1ε, which serve as quantitative metrics for assessing the uniformity of the crystalline network. SANS, on the other hand, offers high sensitivity to structural nuances, particularly through analyses based on Guinier and Porod regimes. This technique can elucidate details of crystallite morphology, such as relative packing and surface roughness, thereby further refining our understanding of how nanoscale order contributes to overall chocolate quality.

At the mesoscale, USAXS bridges the gap between the nanoscale features captured by SAXS/SANS and the macroscopic properties of the final product. USAXS extends the accessible scattering range, allowing us to quantify larger-scale heterogeneities, domain structures, and long-range correlations in chocolate. This technique yields key parameters—specifically correlation lengths and fractal dimensions—that offer insights into the evolution of the chocolate's crystal network during cooling and solidification. Distinct slope ranges in the scattering data should be utilized, the first slope, observed in the low-q region, corresponds to larger-scale structures. The second, in the high-q region, reflects the finer microstructural features. Notably, properly tempered CB exhibits a high target value in both the high-q slope range and low-q slope range close to −4—a signature characteristic that must be maintained as a control when analyzing suspect samples where an untempered or impurely tempered chocolate display high variance and value anywhere from −2 to −3.5. Any deviation from this high range may indicate a departure from optimal tempering. Moreover, a diffraction peak at approximately 690 nm maybe used a marker of well-tempered CB. This peak reinforces the notion that both slope metrics and specific diffraction features are essential for evaluating the structural nuances of CB in chocolate. By using a properly tempered CB as a benchmark, deviations in either the slope ranges or the diffraction peak can serve as a robust quality control metric, and deviation may imply an improperly tempered chocolate.

Finally, SR-μCT serves as the macroscopic validation tool in our multiscale framework. SR-μCT provides a nondestructive, three-dimensional visualization of the chocolate's internal architecture, revealing the distribution of air pockets, density variations, and any defects that might compromise quality such as cracking. Although SR-μCT lacks the resolution of scattering techniques, its strength lies in capturing the cumulative effects of molecular, nanoscale, and mesoscale processes. For example, the identification of high-density regions and potential crack initiation sites in SR-μCT images can be correlated with earlier observations from scattering analyses, thus offering a quantitative quality control metric.

The real strength of this multiscale approach lies in its integrative nature. By correlating data across IR, WAXS, SAXS, SANS, USAXS, and SR-μCT, researchers can construct a comprehensive timeline of the crystallization process. Initial molecular interactions, as detected by IR, inform the development of nanostructures captured by WAXS, SAXS, and SANS. These nanoscale features then evolve into mesoscale architectures observed via USAXS, which ultimately manifest as the macroscopic characteristics visible through SR-

https://doi.org/10.1021/acs.cgd.5c00269
Cryst. Growth Des. 2025, 25, 2764−2783

μCT. In doing so, we not only challenge the traditional paradigm that focuses solely on polymorphic form but also establish actionable metrics—such as lamella spacing, crystallite size, microstrain, and fractal dimensions—that collectively define the essence of proper tempering. Our refined multiscale framework not only links analytical techniques to specific structural parameters—from molecular interactions to macroscopic integrity—but also paves the way for innovative processing strategies that reduce energy costs, simplify production, and enhance product quality. Building on our refined approach to quality assessment, it is crucial to now examine how current challenges in CB sourcing and market pressures may compromise the consistency of supplied CB required for optimal tempering, and how this multiscale understanding can be leveraged to tackle potential ramifications of poor-quality CB.

CURRENT ISSUES IN COCOA BUTTER SOURCING AND POTENTIAL RAMIFICATIONS

The global cocoa industry is facing an unprecedented crisis, with cocoa prices soaring due to a convergence of environmental, economic, and market forces. As cocoa shortages intensify, concerns mount over the long-term availability and quality of CB for chocolate manufacturing. This section explores the key factors driving the crisis and argues that declining CB quality could exacerbate tempering challenges, increasing the risk of fat bloom and instability in chocolate products.

The cocoa supply crisis has emerged due to multiple compounding factors, including declining production in west Africa, leading farmers to abandon cocoa for more profitable crops and causing skyrocketing prices, further fueled by market speculation. West Africa, which produces approximately 60% of the world's cocoa, is experiencing severe production shortfalls due to climate change, disease outbreaks, and aging cocoa trees. In the Ivory Coast, a prolonged dry season has resulted in poor bean quality and lower yields, with farmers reporting stress-induced premature leaf drop due to drought conditions.[81] Similarly, Ghana's cocoa production has dropped to a 20-year low, primarily due to swollen shoot disease (SSD), which now affects 31% of the country's cocoa-growing land—nearly double the 2017 infection rate.[82]

These challenges have driven global cocoa prices to record highs, surging from $4415 per metric ton in January 2024 to over $11 000 per metric ton by early 2025.[83] Speculative trading has further exacerbated price volatility, making cocoa increasingly inaccessible for many chocolate manufacturers.[83] Projections indicate global cocoa deficits may exceed 500 000 t in the coming years. Despite these record prices, many farmers in Ghana and Ivory Coast are abandoning cocoa farming in favor of more resilient crops such as palm oil, rubber, and cassava, which require less labor and withstand climate variability more effectively.[84] Government policies, including fixed farmgate pricing, have prevented farmers from benefiting from rising global prices, driving them to alternative livelihoods. This exodus is expected to reduce the availability of high-quality CB, pushing manufacturers to source from lower-quality suppliers.

IMPLICATIONS FOR COCOA BUTTER QUALITY AND CHOCOLATE STABILITY

As CB shortages worsen, manufacturers may need to source CB from regions with lower quality standards, leading to inconsistencies in fat composition. This shift has major implications directly tied to the central argument of this perspective. Minor lipid components, including phospholipids, play a crucial role in CB crystallization. When manufacturers are forced to extract every last drop of CB from available sources, phospholipid concentrations may increase, and in many cases, chocolate manufacturers use unrefined CB that has a high concentration of FFAs and phospholipids to decrease the yield and eliminate the refining loss that may alter nucleation dynamics, reducing crystal homogeneity, and accelerating bloom formation in the final product.

Our previous work demonstrated that while DMPC promotes Form V crystallization, it also introduces structural defects due to micelle formation, increasing bloom risk. If CB suppliers provide CB with elevated phospholipid content due to inconsistent sourcing or altered manufacturing practices, or poor agronomic practices, chocolate manufacturers may face higher rates of bloom-related defects and product instability, leading to costly consequences. Traditional tempering methods rely on a consistent CB composition to drive the formation of the desirable Form V polymorph during well-established tempering procedures. However, fluctuations in major and minor fat compositions alter nucleation rates—potentially accelerating, delaying, or misdirecting crystallization. This, in turn, affects crystal growth and size distribution, increasing the likelihood of larger, strain-prone crystallites and microstructural instability, ultimately exacerbating fat migration and long-term bloom formation.

These concerns reinforce the argument that another crisis could emerge due to shifts in minor lipid composition in CB supplied to chocolate manufacturers. This further supports the view that polymorphism alone is insufficient to ensure chocolate stability—the multiscale approach to quality assurance put forward is necessary. If manufacturers are forced to work with inconsistent CB quality, they may face increased batch failures due to poor tempering outcomes, higher rejection rates from visible bloom formation during storage, reduced shelf life, and increased reformulation costs to compensate for variable CB behavior. These challenges could significantly impact large-scale chocolate producers, particularly those reliant on strict tempering protocols for mass production, forcing companies to reformulate recipes, adjust processing conditions, or seek novel emulsifiers to counteract CB inconsistencies—all of which increase costs, and, as our literature review has shown, many have failed.

FORWARD THINKING TO ADDRESSING THE CHALLENGE: THE NEED FOR A MULTISCALE APPROACH

Given the growing instability in CB sourcing, a paradigm shift in tempering science is required. Manufacturers must move beyond Form V as the sole quality benchmark and integrate advanced microstructural analysis techniques not only to monitor and control crystallization dynamics, but to fundamentally understand them. Key strategies include utilizing advanced scattering techniques such as (U)SAXS/(U)SANS to analyze nanoscale and microscale CB properties, detecting structural irregularities in the crystallization before

https://doi.org/10.1021/acs.cgd.5c00269
Cryst. Growth Des. 2025, 25, 2764−2783

they are used in a chocolate product and subsequent bloom develops ruining large batches of chocolate. The exploration of the use of phospholipid modifications to regulate nucleation kinetics, reducing the reliance on complex tempering procedures can be taken advantage of rather than causing issues may be possible.

Our recent findings with DMPE as a nucleation agent present a promising path forward, demonstrating that targeted molecular and physical interactions can stabilize CB microstructure even under variable processing conditions. This highlights the necessity of engineering crystallization beyond mere polymorphic identification, ensuring long-term stability despite increasing CB quality variability. A multiscale approach incorporating molecular, microstructural, and processing-level insights will be essential in safeguarding chocolate quality in an era of unpredictable CB supply.

The ongoing cocoa supply crisis is not just a pricing issue—it is a structural challenge that is already reshaping the global chocolate industry. As CB becomes more variable in composition, traditional tempering approaches may fail to deliver stable, bloom-resistant chocolate. This highlights the urgent need to rethink CB crystallization from a multiscale perspective, incorporating advanced characterization techniques and novel nucleation strategies.

By integrating our research on DMPE-tempered chocolate, we can propose new tempering methodologies that account for the evolving challenges in CB sourcing. In doing so, the industry may have a strategy to mitigate waste, production inefficiencies, and the risk of large-scale product instability, ensuring that chocolate manufacturers remain resilient in the face of a volatile cocoa market.

This Perspective serves as both a scientific and industry-relevant call to action—adapting tempering strategies is no longer just about optimizing texture and gloss, but about securing the future stability of chocolate itself in an era of rapid cocoa supply shifts.

■ ASSOCIATED CONTENT

Data Availability Statement

Raw and supporting data will be made available by the authors without reservation.

■ AUTHOR INFORMATION

Corresponding Author

Alejandro G. Marangoni − *Department of Food Science, University of Guelph, Guelph, ON N1G 2W1, Canada;* orcid.org/0000-0002-3129-4473; Email: amarango@uoguelph.ca

Authors

Jarvis A. Stobbs − *Department of Food Science, University of Guelph, Guelph, ON N1G 2W1, Canada; Canadian Light Source, Inc., Saskatoon, SK S7N 2 V3, Canada;* orcid.org/0000-0003-0971-2744

Saeed M. Ghazani − *Department of Food Science, University of Guelph, Guelph, ON N1G 2W1, Canada*

Mary-Ellen Donnelly − *Canadian Light Source, Inc., Saskatoon, SK S7N 2 V3, Canada*

Complete contact information is available at: https://pubs.acs.org/10.1021/acs.cgd.5c00269

Author Contributions

J.A.S. contributed to the planning and execution of all experimental procedures, data collection, analysis and the writing of the manuscript. S.M.G contributed to the execution of all DSC procedures, XRD data collection and writing of the manuscript. M-E.D. contributed to the analysis of all (U)SAXS and SANS data. A.G.M. contributed to the experimental planning, carried out SANS experiments and contributed to the writing of the manuscript.

Notes

The authors declare no competing financial interest.

■ ACKNOWLEDGMENTS

Part of the research described in this paper was performed at the Canadian Light Source, a national research facility of the University of Saskatchewan, which is supported by the Canada Foundation for Innovation (CFI), the Natural Sciences and Engineering Research Council (NSERC), the National Research Council (NRC), the Canadian Institutes of Health Research (CIHR), the Government of Saskatchewan, and the University of Saskatchewan. CT data handling, processing, and analysis on this paper was partially supported by the grant and contribution-funding program of the National Research Council of Canada. Thanks to Kenneth Truong for data collection of USAXS data. J.A.S. would like to acknowledge Angeliki Barlas with assistance in production of graphical abstract image.

■ REFERENCES

(1) Venter, M. J.; Schouten, N.; Hink, R.; Kuipers, N. J. M.; de Haan, A. B. Expression of cocoa butter from cocoa nibs. *Sep. Purif. Technol.* **2007**, *55* (2), 256−64.

(2) Windhab, E. J. Tempering. In *Beckett's Industrial Chocolate Manufacture and Use*; John Wiley & Sons, Ltd, 2017; pp 314−355. Available from: https://onlinelibrary.wiley.com/doi/abs/10.1002/9781118923597.ch13. Accessed Nov. 15, 2021.

(3) Ghazani, S. M.; Marangoni, A. G. Molecular Origins of Polymorphism in Cocoa Butter. *Annu. Rev. Food Sci. Technol.* **2021**, *12* (1), 567−90.

(4) Lutton, E. S. Review of the polymorphism of saturated even glycerides. *J. Am. Oil Chem. Soc.* **1950**, *27* (7), 276−81.

(5) Manning, D., Dimick, P. Crystal Morphology of Cocoa Butter. *Food Struct.* **1985** *4* (2). Available via the Internet at: https://digitalcommons.usu.edu/foodmicrostructure/vol4/iss2/9.

(6) Larsson, K.; Cyvin, S. J.; Rymo, L.; Bowie, J. H.; Williams, D. H.; Bunnenberg, E.; Djerassi, C.; Records, R. Classification of glyceride crystal forms. *Acta Chem. Scand.* **1966**, *20* (8), 2255.

(7) Ghazani, S. M.; Marangoni, A. G. New Insights into the β Polymorphism of 1,3-Palmitoyl-stearoyl-2-oleoyl Glycerol. *Cryst. Growth Des.* **2018**, *18* (9), 4811−4814.

(8) Violato, L. Study of the crystallization behaviour of mixtures of triglycerides for the production of dairy-free chocolate. *Politecnico di Torino*; **2023**. Available via the Internet at: https://webthesis.biblio.polito.it/28131/. Accessed Feb. 28, 2025.

(9) Afoakwa, E. O. *Chocolate Science and Technology*; John Wiley & Sons, 2016; 565 pp.

(10) Wille, R. L.; Lutton, E. S. Polymorphism of cocoa butter. *J. Am. Oil Chem. Soc.* **1966**, *43* (8), 491−496.

(11) Merken, G. V.; Vaeck, S. V. A study of the polymorphism of cacao butter by means of DSC calorimetry. *Lebensm-Wiss Technol.* **1980**, *13* (6), 314−317.

(12) Vaeck, S. V. Cocoa butter and fat bloom. *Manuf. Confect.* **1980**, *40* (35), 71−74.

(13) Hartel, R. W. Chocolate: Fat Bloom During Storage. *Manuf. Confect.* **1999**, 89−99.

(14) Marty, S.; Marangoni, A. G. Effects of Cocoa Butter Origin, Tempering Procedure, and Structure on Oil Migration Kinetics. *Cryst. Growth Des.* **2009**, *9* (10), 4415−4423.
(15) Becker, K. Über die Fettreif-Bildung bei Schokoladen und Pralinen I. *Fette Seifen Anstrichm.* **1957**, *59* (8), 636−44.
(16) Kleinert, J. Studies on the formation of fat bloom and the methods of delaying it. In *15th Pennsylvania Manufacturing Confectioners Association Production Conference*, Lancaster, PA; 1961; pp 386−399.
(17) Schlichter-Aronhime, J.; Garti, N. Solidification and polymorphism in cocoa butter and the blooming problems. *Cryst. Polymorph Fats Fat Acids* **1988**, *31*, 363−393.
(18) Kinta, Y, Hatta, T. 8 - Morphology of Chocolate Fat Bloom. In *Cocoa Butter and Related Compounds*; Garti, N, Widlak, N. R., Eds.; AOCS Press, 2012; pp 195−212. Available via the Internet at: https://www.sciencedirect.com/science/article/pii/B9780983079125500116. Accessed Feb. 12, 2024.
(19) Sato, K, Koyano, T. Crystallization Properties of Cocoa Butter. In *Crystallization Processes in Fats and Lipid Systems*. CRC Press, 2001.
(20) Bricknell, J.; Hartel, R. W. Relation of fat bloom in chocolate to polymorphic transition of cocoa butter. *J. Am. Oil Chem. Soc.* **1998**, *75* (11), 1609−15.
(21) Kinta, Y.; Hatta, T. Composition and Structure of Fat Bloom in Untempered Chocolate. *J. Food Sci.* **2005**, *70* (7), s450−2.
(22) Kinta, Y.; Hartel, R. W. Bloom Formation on Poorly-Tempered Chocolate and Effects of Seed Addition. *J. Am. Oil Chem. Soc.* **2010**, *87* (1), 19−27.
(23) Othmer, K. Über die Einwirkung von Phosphoroxychlorid auf die Natriumsalze organischer Säuren. *Z. Für Anorg Chem.* **1915**, *91*, 240.
(24) Clarkson, C. E.; Malkin, T. Alternation in long-chain compounds. Part II. An X-ray and thermal investigation of the triglycerides. *J. Chem. Soc. (Resumed)* **1934**, 666−671.
(25) deMan, J. M. Microscopy in the Study of Fats and Emulsions. *Food Struct.* **1982** *1* (2). Available via the Internet at: https://digitalcommons.usu.edu/foodmicrostructure/vol1/iss2/10.
(26) Haighton, A. J. The measurement of the hardness of margarine and fats with cone penetrometers. *J. Am. Oil Chem. Soc.* **1959**, *36* (8), 345−348.
(27) Lovegren, N. V.; Guice, W. A.; Feuge, R. O. An instrument for measuring the hardness of fats and waxes. *J. Am. Oil Chem. Soc.* **1958**, *35* (7), 327−331.
(28) Ravich, G. B.; Volnova, V. A. *Acta Physicochim. URSS.* **1942**, *17*, 323−336.
(29) von Rosenberg, G. Frhr. Messung der Härte von Wachsen. *Fette Seifen Anstrichm.* **1954**, *56* (4), 214−218.
(30) Davidge, R. W.; Green, T. J. The strength of two-phase ceramic/glass materials. *J. Mater. Sci.* **1968**, *3* (6), 629−634.
(31) Afoakwa, E. O.; Paterson, A.; Fowler, M.; Vieira, J. Effects of tempering and fat crystallisation behaviour on microstructure, mechanical properties and appearance in dark chocolate systems. *J. Food Eng.* **2008**, *89* (2), 128−136.
(32) Chen, J.; Ghazani, S. M.; Stobbs, J. A.; Marangoni, A. G. Tempering of cocoa butter and chocolate using minor lipidic components. *Nat. Commun.* **2021**, *12* (1), 5018.
(33) Nedomova, S.; Trnka, J.; Buchar, J. Tensile Strength of Dark Chocolate. *Acta Technol. Agric.* **2013**, *16* (3), 71−73.
(34) Declerck, A.; Nelis, V.; Danthine, S.; Dewettinck, K.; Van der Meeren, P. Characterisation of Fat Crystal Polymorphism in Cocoa Butter by Time-Domain NMR and DSC Deconvolution. *Foods* **2021**, *10* (3), 520.
(35) A Raman Spectroscopic Method of Evaluating Fat Crystalline States and Its Application in Detecting Pork Fat. Available via the Internet at: https://www.jstage.jst.go.jp/article/jarq/52/1/52_17/_article/-char/ja/. Accessed Feb. 3, 2025.
(36) Yano, J.; Sato, K. FT-IR studies on polymorphism of fats: molecular structures and interactions. *Food Res. Int.* **1999**, *32* (4), 249−59.
(37) Hodge, S. M.; Rousseau, D. Fat bloom formation and characterization in milk chocolate observed by atomic force microscopy. *J. Am. Oil Chem. Soc.* **2002**, *79*, 1115 (Accessed Feb. 3, 2025).
(38) Narayanan, T.; Wacklin, H.; Konovalov, O.; Lund, R. Recent applications of synchrotron radiation and neutrons in the study of soft matter. *Crystallogr. Rev.* **2016**, *23* (3), 160−226 (Accessed Feb. 3, 2025).
(39) Feng, C. H.; Otani, C.; Hoshina, H. Characterization of Different Types of Crystallization from Cocoa Butter by Using Terahertz Spectroscopy. *Appl. Sci.* **2024**, *14* (1), 35.
(40) Oil migration: Novel approaches to a familiar problem. *Lipid Technol.* **2014**, *26* (11−12), 243−245.
(41) Peyronel, F.; Ilavsky, J.; Pink, D. A.; Marangoni, A. G. Quantification of the physical structure of fats in 20 minutes: Implications for formulation. *Lipid Technol.* **2014**, *26* (10), 223−226.
(42) Bayés-García, L.; Patel, A. R.; Dewettinck, K.; Rousseau, D.; Sato, K.; Ueno, S. Lipid crystallization kinetics—roles of external factors influencing functionality of end products. *Curr. Opin. Food Sci.* **2015**, *4*, 32−38.
(43) Ghazani, S. M.; Marangoni, A. G. New Triclinic Polymorph of Tristearin. *Cryst. Growth Des.* **2023**, *23* (3), 1311−1317.
(44) Kinta, Y., Hatta, T. 8 - Morphology of Chocolate Fat Bloom. In *Cocoa Butter and Related Compounds*; Garti, N., Widlak, N. R., Eds.; AOCS Press, 2012; pp 195−212. Available from: https://www.sciencedirect.com/science/article/pii/B9780983079125500116. [cited 2024 Feb 12]
(45) Tietz, R. A.; Hartel, R. W. Effects of minor lipids on crystallization of milk fat-cocoa butter blends and bloom formation in chocolate. *J. Am. Oil Chem. Soc.* **2000**, *77* (7), 763−771.
(46) Talbot, G.; Smith, K.; Bhaggan, K. Influence of minor components on fat crystallization. *Lipid Technol.* **2012**, *24* (4), 83−85.
(47) Duck, W. N. A study of viscosity increase due to solid fat formation in tempering chocolate coatings. *Manuf. Confect.* **1958**, *38*, 9−12.
(48) Duck, W. N. A method to measure the percent solid seed crystals in tempered chocolate. *Manuf. Confect.* **1963**, *43*, 39.
(49) Kleinert, J. Cocoa butter and chocolate: The correlation between tempering and structure. *Rev. Int. Choc.* **1970**, *25*, 386−399.
(50) Hettich, A. Experimental basis for the definiation of "proper" chocolate temper. *Manuf. Confect.* **1966**, *46*, 29−36.
(51) Campbell, L. B.; Keeney, P. G. Temper level effeccts on fat bloom formation on dark chocolate coatings. *Food Technol.* **1968**, *22* (9), 1150.
(52) Wright, A. J.; Hartel, R. W.; Narine, S. S.; Marangoni, A. G. The effect of minor components on milk fat crystallization. *J. Am. Oil Chem. Soc.* **2000**, *77* (5), 463−475.
(53) Wright, A. J.; Marangoni, A. G. Effect of DAG on milk fat TAG crystallization. *J. Am. Oil Chem. Soc.* **2002**, *79* (4), 395−402.
(54) Wright, A j.; Marangoni, A g. The Effect of Minor Components on Milk Fat Microstructure and Mechanical Properties. *J. Food Sci.* **2003**, *68* (1), 182−186.
(55) Hachiya, I.Seeding effects on solidification behavior of cocoa butter and dark chocolate. I. Kinetics of solidification. *J. Am. Oil Chem. Soc.* **1989**. Available via the Internet at: https://aocs.onlinelibrary.wiley.com/doi/abs/10.1007/BF02660743. Accessed Feb. 3, 2025.
(56) Koyano, T., Hachiya, I., Sato, K. Fat Polymorphism and Crystal Seeding Effects on Fat Bloom Stability of Dark Chocolate. *Food Struct.* **1990** *9* (3). Available via the Internet at: https://digitalcommons.usu.edu/foodmicrostructure/vol9/iss3/6.
(57) DuRoss, J. W.; Knightly, W. H. Relationship of sorbitan monosterate and polysorbate 60 to bloom resistance in properly tempered chocolate. *Manuf. Confect.* **1965**, *45*, 51.
(58) Ludwig, K. G. Moderne Emulgatoren zur Verzögerung der Fettreifbildung bei Schokolade. *Fette Seifen Anstrichm.* **1969**, *71* (8), 672−678.

https://doi.org/10.1021/acs.cgd.5c00269
Cryst. Growth Des. 2025, 25, 2764−2783

(59) Garti, N.; Schlichter, J.; Sarig, S. Effect of food emulsifiers on polymorphic transitions of cocoa butter. *J. Am. Oil Chem. Soc.* **1986**, *63* (2), 230−236.
(60) Stobbs, J. A.; Pensini, E.; Ghazani, S. M.; Leontowich, A. F. G.; Quirk, A.; Tu, K.; et al. Phospholipid Self-Assembly in Cocoa Butter Provides a Crystallizing Surface for Seeding the Form V Polymorph in Chocolate. *Cryst. Growth Des [Internet].* **2024**, *24*, 2685.
(61) Stobbs, J. A., Marangoni, A. G., Ghazani, S. M. Dimyristoylphosphatidylethanolamine addition during chocolate manufacture promotes proper tempering of the cocoa butter under simple cooling conditions without shear. *Cryst. Growth Des Rev.*.
(62) den Adel, R.; van Malssen, K.; van Duynhoven, J.; Mykhaylyk, O. O.; Voda, A. Fat Crystallite Thickness Distribution Based on SAXD Peak Shape Analysis. *Eur. J. Lipid Sci. Technol.* **2018**, *120* (9), 1800222.
(63) Rondou, K.; De Witte, F.; Penagos, I. A.; Chen, O.; Dewettinck, K.; Van Bockstaele, F. Crystallization behavior of monoglyceride oleogels: A comparison between a fully hydrogenated palm oil and a fully hydrogenated rapeseed oil based monoglycerides. *Eur. J. Lipid Sci. Technol.* **2024**, *126* (7), 2300261.
(64) Koizumi, H.; Kimura, K.; Takagi, M.; Michikawa, S.; Hirai, Y.; Sato, K.; et al. Effect of accumulated strain on fat bloom in CBS-based compound chocolates. *CrystEngComm.* **2023**, *25* (32), 4562−7.
(65) Williamson, G. K.; Hall, W. H. X-ray line broadening from filed aluminium and wolfram. *Acta Metall.* **1953**, *1* (1), 22−31.
(66) Cullity, B. D. *Elements of X Ray Diffraction*; Addison-Wesley Publishing Company, 1956; 531 pp. Available via the Internet at: http://archive.org/details/elementsofxraydi030864mbp. Accessed Feb. 27, 2025.
(67) Paganin, D. M., Pelliccia, D. X-ray phase-contrast imaging: a broad overview of some fundamentals. In *Advances in Imaging and Electron Physics*, Vol. *218*; Hÿtch, M, Hawkes, P. W., Eds.; Elsevier, 2021; Chapter 2, pp 63−158. Available via the Internet at: https://www.sciencedirect.com/science/article/pii/S1076567021000501. Accessed Nov. 9, 2023.
(68) Paganin, D.; Mayo, S. C.; Gureyev, T. E.; Miller, P. R.; Wilkins, S. W. Simultaneous phase and amplitude extraction from a single defocused image of a homogeneous object. *J. Microsc.* **2002**, *206*, 33−40.
(69) Paganin, D.; Gureyev, T. E.; Pavlov, K. M.; Lewis, R. A.; Kitchen, M. Phase retrieval using coherent imaging systems with linear transfer functions. *Opt. Commun.* **2004**, *234* (1), 87−105.
(70) Czapalay, E. S.; Soleimanian, Y.; Stobbs, J. A.; Marangoni, A. G. Plant tissue-based scaffolds filled with oil function as adipose tissue mimetics. *Curr. Res. Food Sci.* **2025**, *10*, 101002.
(71) Dobson, S.; Stobbs, J.; Laredo, T.; Marangoni, A. G. A facile strategy for plant protein fiber formation without extrusion or shear processing. *Innov. Food Sci. Emerg Technol.* **2023**, *86*, 103385.
(72) Willick, I. R., Stobbs, J, Karunakaran, C, Tanino, K. K. Phenotyping Plant Cellular and Tissue Level Responses to Cold with Synchrotron-Based Fourier-Transform Infrared Spectroscopy and X-Ray Computed Tomography. In *Plant Cold Acclimation: Methods and Protocols*; Hincha, D. K., Zuther, E, Eds.; Methods in Molecular Biology, Vol. *2156*; Springer, New York, 2020; pp 141−159, DOI: 10.1007/978-1-0716-0660-5_11 (accessed July 28, 2020).
(73) Sivakumar, C.; Stobbs, J. A.; Tu, K.; Karunakaran, C.; Paliwal, J. Unravelling particle morphology and flour porosity of roller-milled green lentil flour using scanning electron microscopy and synchrotron X-ray micro-computed tomography. *Powder Technol.* **2024**, *436*, 119470.
(74) Sivakumar, C.; Nadimi, M.; Stobbs, J. A.; Karunakaran, C.; Paliwal, J. A comprehensive assessment of microscopic characterization techniques to accurately determine the particle size distribution of roller-milled yellow pea flours. *Powder Technol.* **2024**, *434*, 119374.
(75) Ren, Y.; Stobbs, J. A.; Lee, D. J.; Li, D.; Karunakaran, C.; Ai, Y. Utilizing Synchrotron-Based X-ray Micro-Computed Tomography to Visualize the Microscopic Structure of Starch Hydrogels In Situ. *Biomacromolecules.* **2024**, *25* (6), 3302−11.
(76) Quirk, A.; Lardner, M. J.; Tun, Z.; Burgess, I. J. Surface-Enhanced Infrared Spectroscopy and Neutron Reflectivity Studies of Ubiquinone in Hybrid Bilayer Membranes under Potential Control. *Langmuir.* **2016**, *32* (9), 2225−2235.
(77) Maleky, F.; Smith, A. K.; Marangoni, A. Laminar Shear Effects on Crystalline Alignments and Nanostructure of a Triacylglycerol Crystal Network. *Cryst. Growth Des.* **2011**, *11* (6), 2335−2345.
(78) Maleky, F. Nanostructure and physical properties of cocoa butter crystallized under laminar shear. The University of Guelph, 2013.
(79) Besselink, R.; Stawski, T. M.; Van Driessche, A. E. S.; Benning, L. G. Not just fractal surfaces, but surface fractal aggregates: Derivation of the expression for the structure factor and its applications. *J. Chem. Phys.* **2016**, *145* (21), 211908.
(80) Konar, N.; Palabiyik, I.; Karimidastjerd, A.; Said Toker, O. Chocolate microstructure: A comprehensive review. *Food Res. Int.* **2024**, *196*, 115091.
(81) Dry season in Ivory Coast triggers cocoa shortage fears, farmers say. *Reuters*, 2025. Available via the Internet at: https://www.reuters.com/world/africa/dry-season-ivory-coast-triggers-cocoa-shortage-fears-farmers-say-2025-02-10/. Accessed Feb. 15, 2025.
(82) Angel, M. Cocoa swollen shoot disease worsening in Ghana, poses long-term threat. *Reuters*, 2024. Available via the Internet at: https://www.reuters.com/world/africa/cocoa-swollen-shoot-disease-worsening-ghana-poses-long-term-threat-2024-08-08/. Accessed Feb. 15, 2025.
(83) Rudge, S. Decoding the Global Chocolate Crisis. *Food Chain Mag.* **2024**. . Available via the Internet at: https://foodchainmagazine.com/news/decoding-the-global-chocolate-crisis/, accessed Feb. 15, 2025.
(84) Wexler, A. Cocoa Farmers Uproot Their Plants Despite Record Prices. *Wall Street J.* **2025**. Available via the Internet at: https://www.wsj.com/finance/commodities-futures/africa-cocoa-production-prices-reseeding-e4d19821. Accessed Feb. 15, 2025.

https://doi.org/10.1021/acs.cgd.5c00269
Cryst. Growth Des. 2025, 25, 2764−2783